AD_____

Award Number:
W81XWH-10-1-0149

TITLE:
Cytoprotection: Immune and Matrix Modulation of Tissue Repair

PRINCIPAL INVESTIGATOR:
Gerald T. Nepom, MD, PhD
Robert B. Vernon, PhD

CONTRACTING ORGANIZATION: Benaroya Research Institute at Virginia Mason
                           Seattle, WA 98101-2795

REPORT DATE: April 2011

TYPE OF REPORT: Annual

PREPARED FOR:
U.S. Army Medical Research and Materiel Command
Fort Detrick, Maryland 21702-5012

DISTRIBUTION STATEMENT:

■ Approved for public release; distribution unlimited

REPORT DOCUMENTATION PAGE			*Form Approved* OMB No. 0704-0188
Public reporting burden for this collection of information is estimated to average 1 hour per response, including the time for reviewing instructions, searching existing data sources, gathering and maintaining the data needed, and completing and reviewing this collection of information. Send comments regarding this burden estimate or any other aspect of this collection of information, including suggestions for reducing this burden to Department of Defense, Washington Headquarters Services, Directorate for Information Operations and Reports (0704-0188), 1215 Jefferson Davis Highway, Suite 1204, Arlington, VA 22202-4302. Respondents should be aware that notwithstanding any other provision of law, no person shall be subject to any penalty for failing to comply with a collection of information if it does not display a currently valid OMB control number. **PLEASE DO NOT RETURN YOUR FORM TO THE ABOVE ADDRESS.**

1. REPORT DATE *(DD-MM-YYYY)* 14/04/2011	2. REPORT TYPE Annual	3. DATES COVERED *(From - To)* 03/15/2010 – 03/14/2011

4. TITLE AND SUBTITLE Cytoprotection: Immune and Matrix Modulation of Tissue Repair	5a. CONTRACT NUMBER
	5b. GRANT NUMBER W81XWH-10-1-0149
	5c. PROGRAM ELEMENT NUMBER
6. AUTHOR(S) Gerald T. Nepom, MD, PHDRobert B. Vernon, PhD jnepom@benaroyaresearch.org	5d. PROJECT NUMBER
	5e. TASK NUMBER
	5f. WORK UNIT NUMBER

7. PERFORMING ORGANIZATION NAME(S) AND ADDRESS(ES) AND ADDRESS(ES) Benaroya Research Institute at Virginia Mason 1201 Ninth Avenue Seattle, WA 98101-2795	8. PERFORMING ORGANIZATION REPORT

9. SPONSORING / MONITORING AGENCY NAME(S) AND ADDRESS(ES) U.S. Army Medical Research and Material Command 1077 Patchel Street Fort Detrick, Maryland 21702-5012	10. SPONSOR/MONITOR'S ACRONYM(S)
	11. SPONSOR/MONITOR'S REPORT

12. DISTRIBUTION / AVAILABILITY STATEMENT
Approved for public release; distribution unlimited

13. SUPPLEMENTARY NOTES

14. ABSTRACT
The research program consists of a set of projects addressing two Aims:(1) to develop and evaluate formulations of natural cytokines, ligands, and extracellular matrix (ECM) components to promote regulatory T-cell (Treg) and macrophage persistence and function, further to control inflammation and improve healing, and (2) to incorporate promising strategies from Aim 1 into a therapeutic device (the *Cytoprotective Implant*, or CI) and test it in an engineered replacement for skeletal muscle (the *myobridge*, also under development in this program). Toward these objectives, significant progress has been made in the following major areas: (1) Novel hyaluronan (HA) ECM hydrogels have been produced that incorporate a number of molecular species to provide potent signals for induction of Treg persistence and function; (2) Small interfering (si)RNAs introduced into naïve human CD4 T-cells were shown to inhibit expression of target genes predicted to affect the generation or stability of Tregs, or inflammatory Th17 T-cells; (3) Beta-2 integrins were implicated as inhibitors of pro-inflammatory responses in a variety of macrophage populations; (4) Inflammatory cytokine blockade with an interleukin 1-receptor antagonist was shown to blunt inflammatory responses in humans; (5) Supportive ECM scaffolds for the CI were evaluated and a novel approach for local, controlled-release of anti-inflammatory HA was developed; and (6) Design and fabrication processes for the myobridge test-bed have been substantially refined.

15. SUBJECT TERMS
Cytoprotection, hydrogels, immune regulation, matrix, myobridge

16. SECURITY CLASSIFICATION OF:			17. LIMITATION OF ABSTRACT	18. NUMBER OF PAGES	19a. NAME OF RESPONSIBLE PERSON USAMRAA
a. REPORT U	b. ABSTRACT U	c. THIS PAGE U	UU	64	19b. TELEPHONE NUMBER *(include area code)*

Standard Form 298 (Rev. 8-98)scribed
by ANSI Std. Z39.18

1. INTRODUCTION

Subject, purpose, and scope of the research

Recent advances in molecular and cellular biology offer an opportunity to create new therapies to regulate tissue reparative processes through the use of specific extracellular matrix (ECM) components, which play a significant role in regulating the inflammatory processes that follow injury, creating cytoprotective environments that promote healing. Prior to the current project, the Benaroya Research Institute's Center for Inflammation and Tissue Repair (CITR) developed a number of tissue repair strategies that utilized engineered ECM scaffolds comprised of proteoglycans and natural collagen, which emphasized enhancement of elasticity, strength, cellular survival and orientation, and optimal integration with host tissue. The current research program expands on this prior work to address a key challenge to clinical application of our engineered tissue repair technology–the host inflammatory response. This new program in *cytoprotection* addresses a major barrier to effective cell-based therapies, namely, that, after treatment with regenerating or reconstituted cells or stem cells, the viability of those therapeutic cells is often threatened by the noxious microenvironment of inflamed tissue.

The research program consists of a coordinated set of projects that address two Specific Aims (listed below). The goal of projects in Aim 1 is to develop and evaluate specific cytoprotective modulators of tissue-immune interactions. The goal of Aim 2 is to develop an engineered tissue model (a "myobridge" for replacement of skeletal muscle) and use it as a test-bed to evaluate promising cytoprotective strategies identified in Aim 1 for their capacity to control inflammation, improve cell survival, and promote healing.

Specific Aims

Aim 1   To develop ECM hydrogels with cytoprotective properties, including mechanical resistance to shear, binding sites for specific bioactive molecules, and sites for retention of regulatory lymphocytes. Novel cytoprotective mediators associated with regulatory lymphocytes and innate immune activation will be identified using siRNA (human and mouse) and knockout animal models, and potential biomarkers for monitoring efficacy in humans will be evaluated in a pilot clinical research study.

Aim 2   To use cytoprotective ECM hydrogels in customized skeletal muscle implants to evaluate a novel engineered tissue, referred to as a "myobridge," designed to enable rapid reconstruction of extensive skeletal muscle wounds. Cytoprotection from inflammation-mediated damage, vascularization, and myocyte differentiation within the graft will be evaluated.

2. BODY

2.1. Statement of Work

The research program is two years in duration and is organized into 15 specific Tasks, which are indicated below. Tasks that have activated in Year 1 are indicated by yellow highlight and are the subject of this report.

Specific Aim 1: Cytoprotective Mechanisms of Immune Regulation

Task 1   *(Months 1 – 9)*   Develop and test stable, shear-resistant HMW-HA/fibrillar collagen hydrogels on dye-cut 2.9 mm nylon mesh rings.

Task 2   *(Months 2 – 12)*   Validate microwell plate assay for expression using murine T cells and hydrogel rings at collagen:HMW:HA ratios of 8:1, 4:1, 2:1, 1:1, 1:2, 1:4, and 1:8.

Task 3 *(Months 6 – 18)* Supplement hydrogel microwell GFP-FOXP3 assay with rapamycin, IL-10, and TGF-β, with and without gelatin sponge component.

Task 4 *(Months 1 – 12)* Perform flow cytometry assays for lineage deviation with 11 siRNA constructs (listed in the proposal) using human naïve CD4 T cells.

Task 5 *(Months 12 – 24)* Evaluate *in vivo* candidate siRNA using DO11.10-Treg transfection.

Task 6 *(Months 1 – 8)* Evaluate siRNA for TREM-2 and DAP12 for inhibition of TNF production by THP-1 cells.

Task 7 *(Months 6 – 24)* Measure TLR activation by cytokine production and phospho-specific antibodies in CD18 and BCAP KO mice, and map BCAP domains as potential therapeutic targets.

Task 8 *(Months 6 – 24)* Measure serum biomarkers in 20 human subjects treated with IL1RA after inflammatory stimulus.

Specific Aim 2: The CITR Cytoprotective Implant (CI) and Myobridge

Task 9 *(Months 3 – 12)* Production of the three-layer CI "sandwich".

Task 10 *(Months 6 – 16)* Evaluation of prototype CI in rat dermal pockets for histological monitoring of biodegradation and in mouse dermal pockets for evaluation of regulatory T cell responses.

Task 11 *(Months 1 – 12)* Development of myobridges using uniaxial supports and collagen gels populated with myoblastic cells. Histological evaluation of cultured myobridges for cell survival, new muscle cell generation, proliferation, and differentiation.

Task 12 *(Months 12 – 24)* Implantation of cell-seeded myobridge into female F344 rat anterior tibialis, with histological analysis after 3 weeks.

Task 13 *(Months 12 – 24)* Supplementation of myobridge with CoPP and regulatory modulators from Aim 1, prior to implantation.

Task 14 *(Months 16 – 24)* Co-transplantation of myobridge and CI to evaluate effects of CI-mediated immunomodulation on integration of the myobridge with host tissues.

Task 15 *(Months 18 – 24)* *In vitro* seeding of myobridge prototypes with human MDSC for evaluation of human cell compatibility with hydrogel components.

2.2. Research Accomplishments for Year 1

Note: Figures are numbered sequentially for each Task.

Tasks 1, 2, and 3

Tasks 1, 2, and 3 are components of Aims 1A and 1B which focus on development of high molecular weight hyaluronan (HMW-HA)-based hydrogels which will be engineered for controlled release of growth factors and cytokines. HMW-HA is a polysaccharide glycosaminoglycan (GAG) found in many tissues, which has natural cytoprotective and wound repair-promoting properties. HMW-HA is associated with tissue repair as a consequence of its unique mechano-chemical properties (e.g., a hygroscopic character, viscoelasticity, and high negative charge) and its ability to modulate cell behavior by interacting with other ECM molecules or with specific cell surface receptors. Early response to tissue injury includes the formation of a provisional ECM rich in HMW-HA and fibrin, which supports fibroblastic invasion and penetration of new blood vessels into the wound site. Our laboratories have recently described a novel anti-inflammatory mechanism for HA, in which HMW-HA acts as a costimulator of regulatory T cell (Treg) activation through binding of CD44v6, resulting in persistence of FOXP3 gene expression, a transcriptional regulator, which promotes maintenance of the regulatory phenotype. In Aim 1, we evaluate different approaches to retain HMW-HA in the wound or graft site for ultimate inclusion in our cytoprotective implant (Aim 2).

Task 1 Develop and test stable, shear-resistant HMW-HA/fibrillar collagen hydrogels on dye-cut 2.9 mm nylon mesh rings (Robert Vernon, PhD).

For Task 1, we have evaluated the capacity of HMW-HA/fibrillar collagen hydrogels to adhere to nylon mesh rings as a basis for the microwell plate assay described in Task 2. The rings chosen are dye-cut from nylon (Nitex) mesh with a mesh weave of 100 micron square spacing providing an open space of 44% per unit area of mesh. This material is wettable by the hydrogel prior to crosslinking, meaning that the hydrogel will intercalate into the open spaces of the mesh to provide stable mechanical attachment. We have observed that hydrogels with relatively high ratios of collagen adhere better than hydrogels with relatively high ratios of HMW-HA. Generally, adhesion of ECM hydrogels to woven mesh materials can be improved by increasing the mesh weave spacing; however, meshes that are excessively coarse have a propensity to unravel at the die cut edges, which can be a problem with small-diameter rings like the ones used here. We have determined that 100 micron mesh/44% open space nylon (Nitex) mesh works adequately. In addition to Nitex nylon meshes, we also evaluated open-pore polyvinyl alcohol (PVA) sponge materials of various pore sizes. The 3-dimensional labyrinth of pores within these materials may provide a significantly larger area for attachment of ECM hydrogels than standard nylon mesh, but without the associated problem of physical instability. We determined that PVA sponge with an average 90 micron pore diameter will support HMW-HA hydrogels adequately. Task 1 has been completed.

Task 2 Validate microwell plate assay for expression using murine T cells and hydrogel rings at collagen: HMW:HA ratios of 8:1, 4:1, 2:1, 1:1, 1:2, 1:4, and 1:8 (Gerald Nepom, MD, PhD).

We completed studies of the microwell plate assay system for evaluating effects on GFP/FOXP3 induction in murine T cells. We first evaluated the Wallace Victor plate reader and the Packard Fusion fluorescence imager for their ability to discriminate levels of fluorescence seen with titrations of CD4+GFP/FOXP3+ sorted Treg or CFSE-labeled CD4+ T cells. The Packard fluorescence imager had by far greater sensitivity. Using this apparatus, we evaluated a variety of clear plastic cell culture systems. We found that only specifically-designed fluorescence analysis plates had low enough backgrounds to allow us to discriminate levels of fluorescence seen with titrations of CD4+GFP/FOXP3+ sorted Treg or fluorescently (CFSE)-labeled CD4+ T cells. Within this system, using fixed CFSE-labeled CD4+ T cells, we found no difference in the ability to detect fluorescence by cells: (a) embedded within hydrogels, (b) plated on top of hydrogels, or (c) plated on plastic alone without hydrogels present. Notably, however, the fluorescence analysis plates adversely affected the viability of CD4+GFP/FOXP3+ sorted Treg, as well as CFSE-labeled CD4+ T cells, such that all cells cultured with these plates were dead (as indicated by 7AAD/Annexin V positivity) within 48 hours. This effect on cell viability indicates that use of this system as a high-throughput assay for GFP/FOXP3 expression remains to be fully worked out. Accordingly, we shifted our analytical approach towards conventional flow-cytometry methods, with which we have extensive experience.

To use conventional flow cytometry to measure expression of GFP/FOXP3 by T cells cultured in 3-dimensional ECM hydrogels, the cells must be rapidly released from the gels for assay. To facilitate cell release, we evaluated Extracel-SS™, an HMW-HA hydrogel available from Glycosan Biosystems (Salt Lake City, UT) that incorporates a novel PEGSSDA crosslinker. PEGSSDA can be cleaved with low concentrations of disulfide bond reducing agent, thereby permitting liquefaction of the hydrogel for cell release while avoiding damage to the cells. In all other respects, this hydrogel biomaterial is identical to the HMW-HA formulation described in the original application. Using Extracel-SS as a support medium in combination with conventional flow cytometry, we have established that a 2:2:1 ratio of HMW-HA:collagen (gelatin):PEGSSDA crosslinker induces the highest levels of GFP/FOXP3 expression by cultured Treg. This ratio is the same as that recommended for lymphocyte work by the manufacturer and is the formulation that we have based our subsequent studies for Task 3. Task 2 has been completed.

Task 3 Supplement hydrogel microwell GFP-FOXP3 assay with rapamycin, IL-10, and TGF-β, with and without gelatin sponge component (Gerald Nepom, MD, PhD).

As mentioned in the narrative for Task 2 above, we found it was not possible to use the microwell format to analyze GFP/FOXP3 induction results and, therefore, we switched to flow cytometry-based analysis. Using this approach, we evaluated the effects of gelatin sponge inclusion on FOXP3 induction. We have found that the gelatin sponge adds structural integrity to the gel such that it can be manipulated for assay. However, upon the inclusion of T cells in the hydrogel, the gelatin sponge is degraded within 3-4 days, indicating that these cells produce collagenases. The gelatin sponge appears to have no discernable impact on FOXP3 induction, perhaps because there is already gelatin in the Extracel HA hydrogel preparation. In sum, these data suggest to us that the gelatin sponge adds structural integrity to hydrogels polymerized *in vitro* and that there is no functional disadvantage vis-à-vis FOXP3 induction to having the gelatin sponge present.

Subsequently, we developed methods to evaluate the capacity of hydrogels to incorporate cytokines to stimulate FOXP3 expression by T cells. For these experiments, we used Extracel-HP™ HMW-HA hydrogel, which contains heparin that can bind to a variety of heparin-binding growth factors, including the ILs and TGF-β. We began this work looking at IL-2 and evaluated the capacity of our hydrogel preparation to retain this cytokine over 14 days. We found that for gels of 200 µl volume incubated in media containing 20,000 pg of IL-2, the average total IL-2 stored by the gel at the end of 14 days for three experiments was 12,742 pg, with a standard deviation of 8%. This was equivalent to a retention rate of at least 63% of the original IL-2 loaded into the gel. Importantly, at the end of 14 days the gels were still releasing IL-2 over baseline, indicating that there is potential for long-term bioactivity. The kinetics of release of IL-2 is shown in **Figure 1**.

Subsequently we performed analogous work examining the kinetics of IL-10 release. We found that for gels of 200 µl volume incubated in media containing 20,000 pg of IL-10, the average total IL-10 stored by the gel at the end of 8 days was 13,341 pg, with a standard deviation of ~6%. This was equivalent to a retention rate of at least 67% of the original IL-10 loaded into the gel. As with IL-2, after 14 days the gels were still releasing IL-10 over baseline (**Figure 2**). These data indicate that the hydrogels can be used as a depot for IL-10 storage and release for biological applications.

In addition to the work to incorporate cytokines, such as IL-2 and IL-10 into HMW-HA hydrogels, we have also devised a method to deliver a TCR ligation using the same hydrogel platform. Streptavidin added to the hydrogel/cytokine mixture allows for incorporation of biotinylated anti-CD3 and anti-CD28 antibodies (Ab) into the hydrogel. The streptavidin/Ab complex provides a stimulatory signal through the TCR complex necessary for TR1 induction. These agents, along with IL-2 and TGF-β, are added to the hydrogel material prior to polymerization of the hydrogel. This hydrogel platform, with its cytokines and
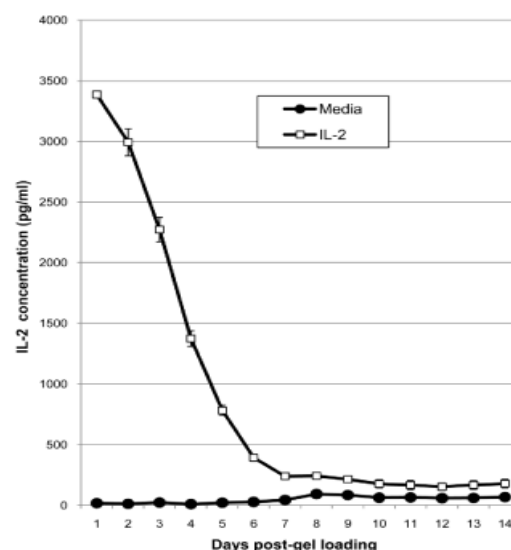
Figure 1. Extracel HP hydrogels release IL-2 over time. Extracel HP gels of 200 µl volume were polymerized and then incubated overnight in 200µl of RPMI containing 1600 IU/ml (20,000 pg) of IL-2. The gel was then washed once in RPMI and incubated in 200 µl of fresh RPMI. The RPMI was removed after 24 hours and stored for subsequent analysis of IL-2 or TGF-β content by ELISA. This process was repeated every 24 hours for 14 days. The experiment was performed three times. One representative experiment is shown.
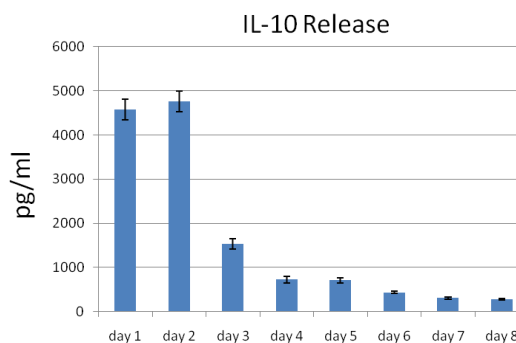
Figure 2. Extracel-HP hydrogels release IL-10 over time. Extracel-HP gels of 200 µl volume were polymerized and then incubated overnight in 200 µl of RPMI containing 20,000 pg of IL-10. The gel was then washed once in RPMI and incubated in 200 µl of fresh RPMI. The RPMI was removed after 24 hours and stored for subsequent analysis of IL-10 content by ELISA. This process was repeated every 24 hours for 8 days. The experiment was performed two times. One representative experiment is shown.

TCR ligation component, can deliver all of the necessary signals to induce FOXP3+ regulatory T-cells. A schematic of this design is shown in **Figure 3A**.

This combination is an exceptionally efficient and innovative system for FOXP3 induction. Starting with conventional T-cell precursors we observed substantial IL-10 production using this hydrogel as a platform for cell culture *in vitro* (**Figure 3B**), but not upon using the same streptavidin/antibody complex incorporated into either Matrigel or a fibrin hydrogel (data not shown). Omission of the HA, but not the collagen, component of the hydrogel abrogated IL-10 production (data not shown). One striking feature of this hydrogel is that the presence of heparan sulfate (HS) dramatically amplified the impact of exogenous TGF-β and IL-2 on induction of FOXP3. This is consistent with reports of altered properties of other cytokines once bound to HS [1,2].
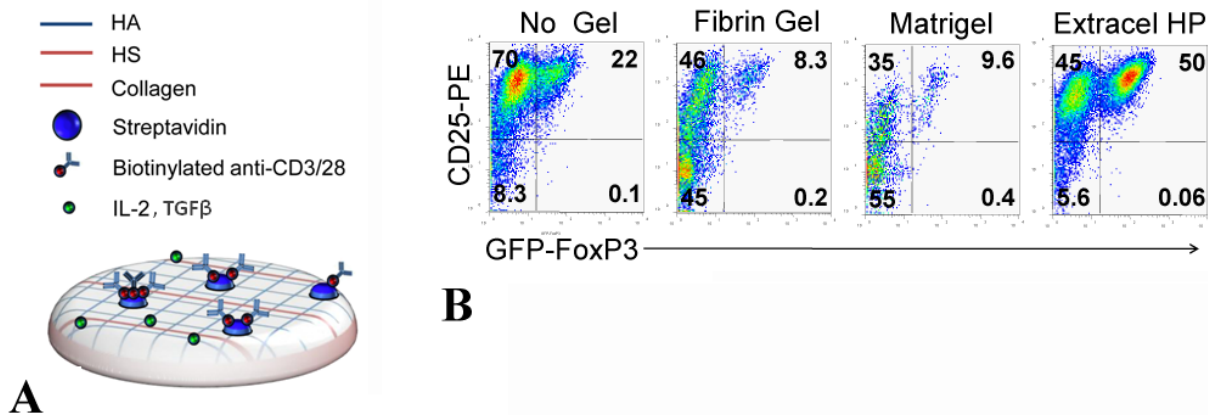
Figure 3. A hydrogel made of crosslinked HA promotes FOXP3 induction. A. *Schematic for the design of a hydrogel capable of delivering a set of cues which we have found potently induces IL-10 production. We used a commercially available hydrogel preparation, Extralink HP, modified in a number of key ways. To provide a TCR signal we have added streptavidin and biotinylated CD3 and CD28 antibodies. We load the gel with recombinant IL-2 at 100 IU/ml and TGF-β at 10 ng/ml. **B.** FOXP3 induction using the Extralink HP-based platform versus no gel, a fibrin gel or Matrigel and the same streptavidin/Ab complexes and the same concentrations of IL-2 and TGF-β.*

References

1. Logeart-Avramoglou, D., Huynh, R., Chaubet, F., Sedel, L., Meunier, A. (2002) Interaction of specifically chemically modified dextrans with transforming growth factor beta1: potentiation of its biological activity. *Biochem. Pharmacol.* **63**: 129-137.
2. Blanquaert, F., Barritault, D., Caruelle, J.P. (1999) Effects of heparan-like polymers associated with growth factors on osteoblast proliferation and phenotype expression. *J. Biomed. Mater. Res.* **44**: 63-72.

Task 4 Perform flow cytometry assays for lineage deviation with 11 siRNA constructs (listed in the proposal) using human naïve CD4 T cells (Jane Buckner, MD).

Task 4 is a component of Aim 1C, which is derived from the finding that the lineage of a naïve CD4 T cell is determined by the cytokine milieu in which it is activated. Recent studies have not only identified multiple CD4 T cell lineages, but have also established that the phenotype of previously committed CD4 T cells can be altered in response to factors in the local environment. Task 4 takes advantage of this information to enhance Treg activation, development, and persistence in engineered ECM hydrogels.

Identification of specific environmental factors that regulate key genetic pathways which, in turn, control T cell behavior may prove to be an effective means to control inflammation and improve wound repair, in conjunction with the HA modulation explored in this project. Aim 1C focuses on a set of 11 genes that we believe are likely to influence T cell function. These target genes code for the cytokines IL-6, IL-23R, and IL-21, the signal transduction factors Stat-1, -3 and -5, PTPN-2 and -22, and the transcription factors FOXP3, RORγt and T-bet.

Task 4 focuses on introducing small interfering (si)RNAs into naïve human CD4 T cells to inhibit expression of the target genes with the goal of identifying pathways for lineage deviation that skew T cell maturation toward regulatory (i.e., Treg) commitment, survival, and function. siRNA inhibition of the target genes is predicted either to affect the generation of T cells with regulatory properties or to stabilize a regulatory phenotype in existing Tregs. In the latter phase of Aim 1C, mouse model systems will be used to determine whether the target genes identify pathways that can be used to manipulate Treg function *in vivo*.

Human subjects approval was granted during Quarter 2, which allowed us to begin experiments. Key experiments to determine an efficient method for introducing siRNAs into lymphocytes revealed that Amaxa nucleofection was the most efficient and least damaging to cells (**Figure 1**). Using 100 pmol of an Alexa 488-conjugated siRNA, we found 97% of cells were transfected using the Amaxa system (**Figure 1B**) without significant cell death, as shown by exclusion of the Viaprobe dye (**Figure 1A**). Given the high efficiency of transfection achieved with Amaxa nucleofection, we predicted that sorting of siRNA-transfected cells would not be required prior to functional analysis of siRNA knockdown.

We selected siRNAs for targeting 6 of the 11 genes proposed in Task 4 (**Table I**). Since siRNAs are known to cause off-target effects related to their primary sequence, we performed all functional analyses using a minimum of two unique sequence siRNAs per target gene. A total of five MISSION siRNAs (Sigma) were to be tested for each target gene to identify at least two siRNAs that could successfully inhibit gene expression. These siRNAs were designed using the Rosetta siRNA design algorithm that maximizes specificity and minimizes off-target effects. Universal negative controls were included in each experiment, as well as two siRNA knockdown positive controls specific for GAPDH and cyclophilin B. Target gene expression was to be assessed by qPCR and Western blot.

In Quarter 3, we adapted and optimized this transfection protocol for primary lymphocytes and confirmed that it resulted in highly efficient transfection, and high viability, in both T cells and B cells isolated from human PBMCs (data not shown). Importantly, the entire population of T or B cells took up siRNA after transfection, precluding, as we predicted, the need for cell sorting of transfected lymphocytes prior to functional assays. We

Figure 1. *Efficient transfection of hematopoietic cells.* A pro-B cell line was mock transfected or transfected with increasing concentrations of an Alexa 488 labeled siRNA using Amaxa nucleofection. Cells were stained with Viaprobe and analyzed by flow cytometry 2h post transfection to assess cell viability (A) and transfection efficiency (B). The percent siRNA transfected cells and the mean fluorescence intensity (MFI) are indicated for each siRNA concentration.

Table I. Sigma MISSION siRNA targets.

Gene target	siRNA start (bp)	Exon	Target sequence	Comment
PTPN2	991	7	GATTCTCATACATGGCTATAA	will repress both
	645	5	AAGTCGTATTATACAGTACAT	isoforms
	651	5	TATTATACAGTACATCTACTA	
	428	3	GGCACAAAGGAGTTACATCTT	
	421	3	TAGAAGAGGCACAAAGGAGTT	
PTPN22	1068	12	CTGAGAAAAATCACACTCTCC	
	616	7	TGAAAAAAGGAAATCTGATTA	
	1640	13	GACTCTAAACACCAAATACGT	
	1406	13	TCTAATTCTAAACCTGTAAAT	
	927	10	GGACACAGAGGCCTTCATTCA	
STAT1	1950	18	TGTTGGGAGAGAAGCTTCTTG	
	1033	9	CAAAATAATAGAGTTGCTGAA	
	1373	11	CCTCAGAGGCCGCTGGTCTTG	
	605	4	TTGGAGAATAACTTCTTGCTA	
	802	6	ACAGAAAGAGCTTGACAGTAA	
STAT3	1029	8	AGAAAACTGGATAACGTCATT	validated siRNA
	1981	19-20	AACGAAGGGTACATCATGGGC	
	1810	17	CAGCTGACTACACTGGCAGAG	
	515	3-4	GCAGGTATCTTGAGAAGCCAA	
	2053	20	ACCTTCCTGCTAAGATTCAGTG	
STAT5A	1967	12	TCCTGTTTGAGTCTCAGTTCA	corepress STAT5A
	2866	20	CCTGACCATGTACTCGATCAG	and STAT5B
	1950	12	AGAGGAGAAGTTCACAGTCCT	
	2887	20	GATGGAGAATTCGACCTGGAT	
	2627	17	ACCTGAGCTATCTCATCTATG	
STAT5B	2196	16	ATGAAGTATACTCCAAATACT	
	1891	14	TGACGGTGTGATGGAAGTATT	
	1490	11	ACAATCCTGTTTGAATCCCAG	
	494	4	ATCCGCCATATSTTGTACAAT	
IL-6	266	2	AGAACGAATTGACAAACAAAT	
	198	2	GCCCCAGTACCCCCAGGAGAAG	
	366	3	GCACTGGCAGAAAACAACCTG	
	246	2	AGACAGCCACTCACCTCTTCA	
	381	3	AACCTGAACCTTCCAAAGAT	

established that an siRNA concentration of 50-100 pmol is optimal to test individual siRNAs for knockdown efficiency in T cells. Higher siRNA concentrations did not result in further knockdown, but did increase off-target effects. We developed qPCR assays to assess gene expression using either SYBR green chemistry or Taqman probes. Expression of siRNA targeted genes was compared relative to expression of the same gene in cells transfected with a negative control siRNA (siRNA that does not recognize human transcripts). A validated siRNA for LAMIN A/C was used as a positive control to confirm transfection efficiency and specificity for
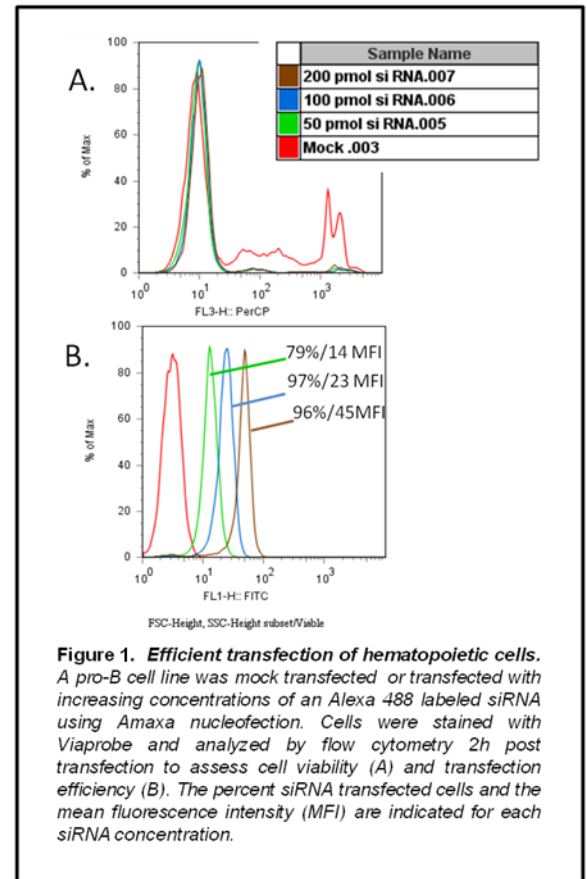
each experiment. Using this optimized protocol, we found that LAMIN A/C expression was reduced by 60-70% in T cells transfected with 100 pmol LAMIN siRNA (not shown).

Subsequently, we tested the knockdown efficiency of a number of gene-specific siRNAs for use in functional experiments, with the goal of identifying two highly effective siRNAs per knockdown target to be able to control for off-target effects. This has been accomplished for the PTPN22 phosphatase in T cells. We found 3 siRNAs that target PTPN22 and result in knockdown greater than 80% by 24 hours post-transfection, and greater than 70% knockdown after 48 hours (**Figure 2**). We identified at least 1 siRNA for the PTPN2 phosphatase that results in 62% knockdown of PTPN2 mRNA in T cells (**Figure 3**).
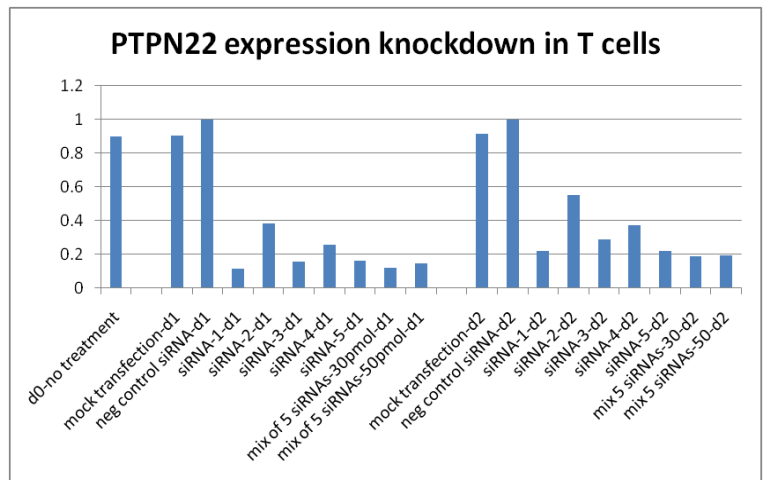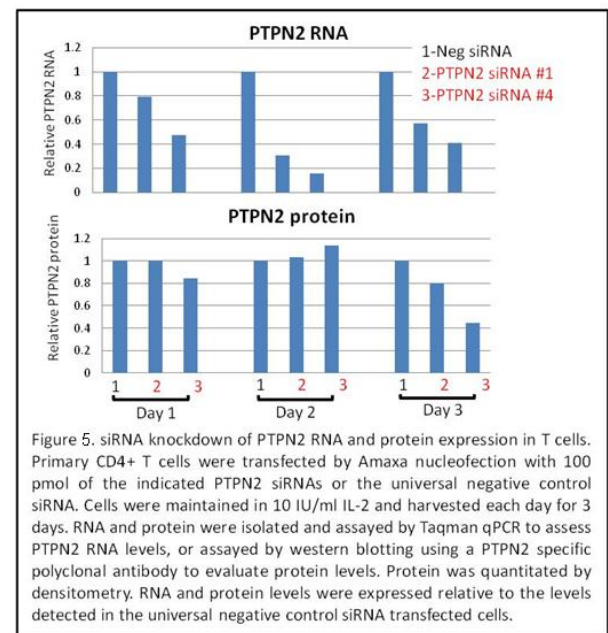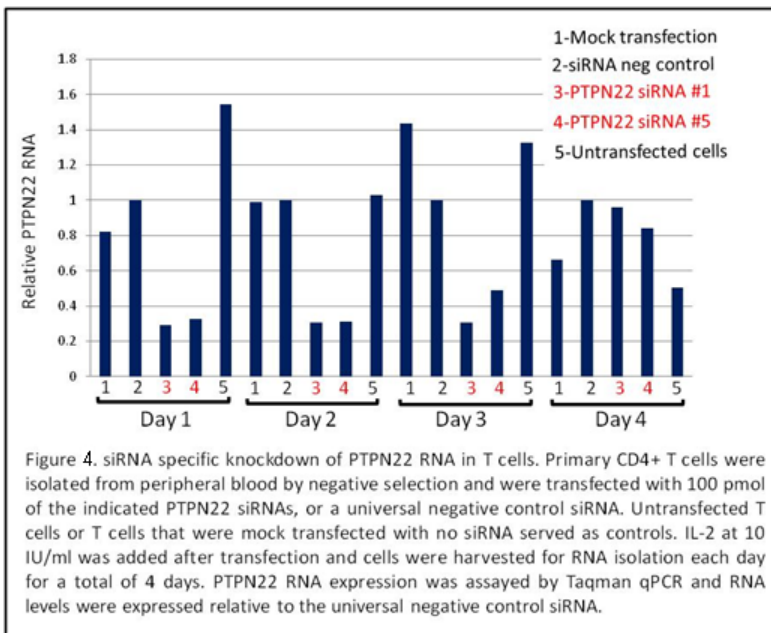

Figure 2. PTPN22 siRNA transfection results in 85-90% knockdown of PTPN22 expression in T cells by 24 hours. Naïve CD4+ T cells transfected with siRNAs using Amaxa Human T Cell Nucleofector Kit and assayed by qPCR for PTPN22 expression after 24 (d1) and 48 (d2) hours. siRNA #1, #3, and #5 result in efficient knockdown of 85-90% by 24 hours, and continued knockdown of 72-78% at 48 hours.

During Quarter 4 we performed additional experiments to validate the time course of siRNA target gene knockdown and quantitate protein reduction. **Figure 4** shows a time course for PTPN22 knockdown at the level of RNA. We found that knockdown of PTPN22 RNA persists through 3 days but by day 4 RNA levels were returning to untransfected cell levels. Similar results were observed for PTPN2 knockdown. We observed that protein knockdown of PTPN2 lags behind RNA knockdown by ~ 48 hours, with detectable knockdown at the protein level observed at 3 days after siRNA transfection (**Figure 5**).
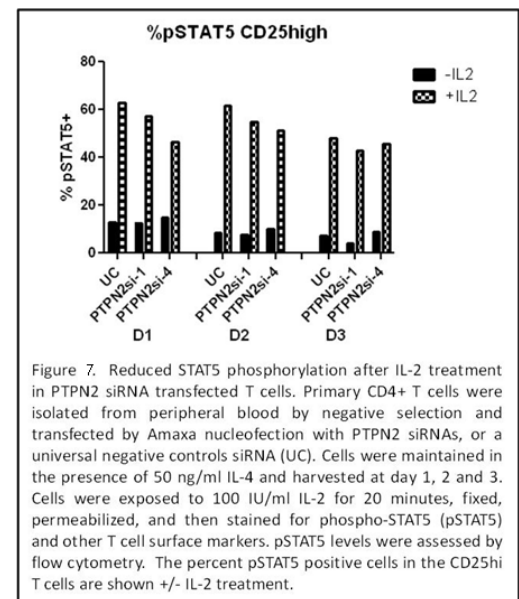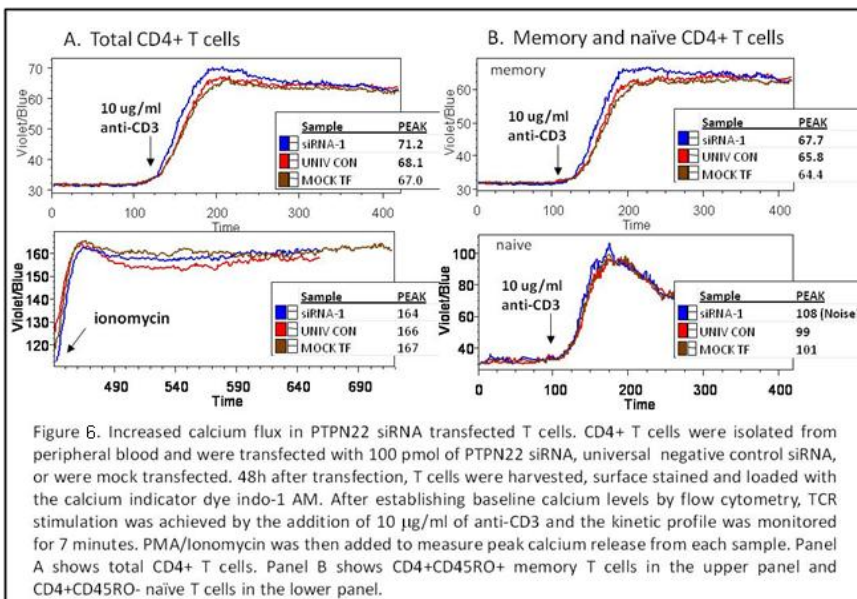
We have begun to evaluate the phenotypic effects of PTPN22 and PTPN2 knockdown in T-cells. We examined T-cell receptor (TCR) signaling in PTPN22 siRNA-transfected T-cells since PTPN22 is known to modulate TCR signal strength. Using calcium flux as a readout of TCR signaling, we observed that PTPN22 siRNA #1 increased the peak calcium flux in T-cells compared to mock or universal negative control siRNA transfected T-cells (**Figure 6**). An increase in calcium flux is the expected result since PTPN22 normally functions to dephosphorylate an activating tyrosine in the active site of the TCR-associated kinase Lck. When we analyzed whether this effect was present in the naïve or memory T-cell subset, we found that the memory, but not naïve, T-cells displayed increased calcium flux. These findings are consistent with our previous results showing that control T-cells, carrying a gain of function mutation in PTPN22, have altered calcium flux in the memory T-cell compartment. These results will be repeated and expanded in Year 2.
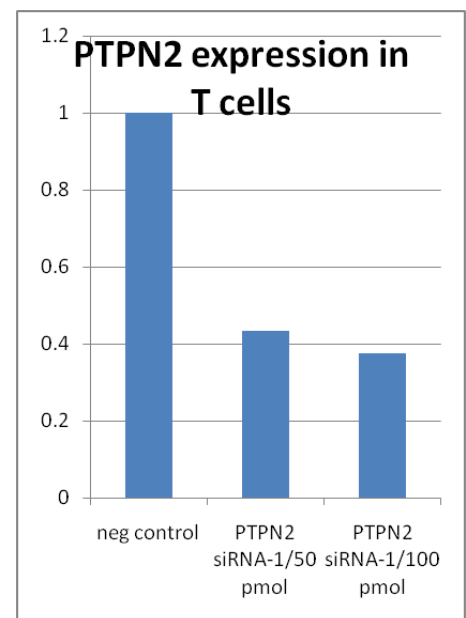
Figure 3. PTPN2 siRNA transfection results in 60% knockdown of PTPN2 expression in T cells. Naïve CD4+ T cells transfected with siRNAs using Amaxa Human T Cell Nucleofector Kit and assayed by qPCR for PTPN2 expression after 48 hours. siRNA #1 transfection (at 50 and 100 pmol) results in approximately 60% knockdown (57% and 63%. respectively) of PTPN2 mRNA compared to a negative control siRNA.

10

Figure 4. siRNA specific knockdown of PTPN22 RNA in T cells. Primary CD4+ T cells were isolated from peripheral blood by negative selection and were transfected with 100 pmol of the indicated PTPN22 siRNAs, or a universal negative control siRNA. Untransfected T cells or T cells that were mock transfected with no siRNA served as controls. IL-2 at 10 IU/ml was added after transfection and cells were harvested for RNA isolation each day for a total of 4 days. PTPN22 RNA expression was assayed by Taqman qPCR and RNA levels were expressed relative to the universal negative control siRNA.

Figure 5. siRNA knockdown of PTPN2 RNA and protein expression in T cells. Primary CD4+ T cells were transfected by Amaxa nucleofection with 100 pmol of the indicated PTPN2 siRNAs or the universal negative control siRNA. Cells were maintained in 10 IU/ml IL-2 and harvested each day for 3 days. RNA and protein were isolated and assayed by Taqman qPCR to assess PTPN2 RNA levels, or assayed by western blotting using a PTPN2 specific polyclonal antibody to evaluate protein levels. Protein was quantitated by densitometry. RNA and protein levels were expressed relative to the levels detected in the universal negative control siRNA transfected cells.
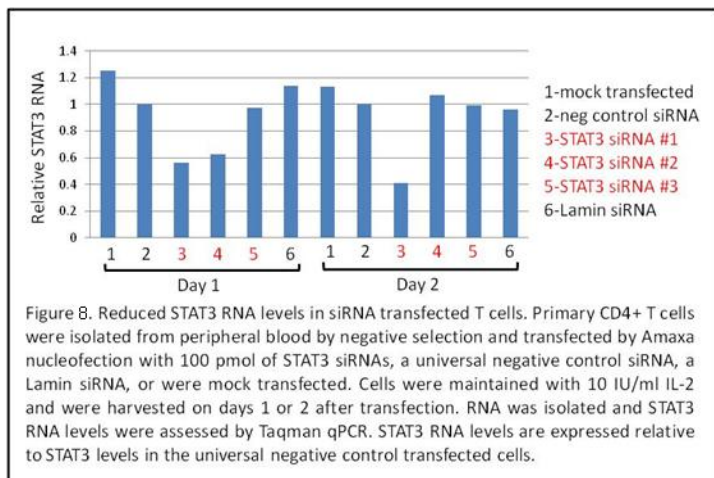
PTPN2 functions to modulate cytokine signaling, including the response to IL-2. To assess the phenotypic effect of PTPN2 knockdown, we examined the phosphorylation of the STAT5 transcription factor (pSTAT5) in the IL-2 pathway after treatment of siRNA-transfected T-cells with IL-2 (**Figure 7**). We observed a reduction in the percentage of pSTAT5-positive cells with both PTPN2 siRNAs, consistent with our previous findings in control subjects carrying a sequence variant that reduces PTPN2 expression. This effect was most evident in the CD25hi fraction of T-cells, which are the most responsive to IL-2. We are currently repeating these results and expanding our analysis to other cytokines known to be modulated by the PTPN2 phosphatase.

Figure 6. Increased calcium flux in PTPN22 siRNA transfected T cells. CD4+ T cells were isolated from peripheral blood and were transfected with 100 pmol of PTPN22 siRNA, universal negative control siRNA, or were mock transfected. 48h after transfection, T cells were harvested, surface stained and loaded with the calcium indicator dye indo-1 AM. After establishing baseline calcium levels by flow cytometry, TCR stimulation was achieved by the addition of 10 μg/ml of anti-CD3 and the kinetic profile was monitored for 7 minutes. PMA/Ionomycin was then added to measure peak calcium release from each sample. Panel A shows total CD4+ T cells. Panel B shows CD4+CD45RO+ memory T cells in the upper panel and CD4+CD45RO- naïve T cells in the lower panel.

Figure 7. Reduced STAT5 phosphorylation after IL-2 treatment in PTPN2 siRNA transfected T cells. Primary CD4+ T cells were isolated from peripheral blood by negative selection and transfected by Amaxa nucleofection with PTPN2 siRNAs, or a universal negative controls siRNA (UC). Cells were maintained in the presence of 50 ng/ml IL-4 and harvested at day 1, 2 and 3. Cells were exposed to 100 IU/ml IL-2 for 20 minutes, fixed, permeabilized, and then stained for phospho-STAT5 (pSTAT5) and other T cell surface markers. pSTAT5 levels were assessed by flow cytometry. The percent pSTAT5 positive cells in the CD25hi T cells are shown +/- IL-2 treatment.

Also in Quarter 4, we expanded our evaluation of siRNAs to new target genes, including STAT3 and the IL-6 receptor. **Figure 8** shows knockdown of RNA levels of the transcription factor STAT3 after transfection of three unique STAT3 siRNAs. One of the STAT3 siRNAs, siRNA #1, was validated as a functional STAT3 siRNA, and it displayed the greatest reduction in STAT3 RNA. STAT3 is a transcription factor that functions in several cytokine pathways including the IL-6 pathway, which is important in the generation of pro-inflammatory Th17 cells. In Year 2, we will assess whether knockdown of STAT3 or IL-6 receptor reduces induction of Th17 cells.

Figure 8. Reduced STAT3 RNA levels in siRNA transfected T cells. Primary CD4+ T cells were isolated from peripheral blood by negative selection and transfected by Amaxa nucleofection with 100 pmol of STAT3 siRNAs, a universal negative control siRNA, a Lamin siRNA, or were mock transfected. Cells were maintained with 10 IU/ml IL-2 and were harvested on days 1 or 2 after transfection. RNA was isolated and STAT3 RNA levels were assessed by Taqman qPCR. STAT3 RNA levels are expressed relative to STAT3 levels in the universal negative control transfected cells.

Collectively, our results show that: (1) our protocol to introduce siRNAs into naïve human CD4 T-cells works and successful transfection of siRNA can result in efficient RNA knockdown, and (2) specific consequences arise from RNA knockdown, which include reduced expression of the cognate protein and effects on cell function that correspond to inhibition of the target genes (e.g., PTPN22, PTPN2).

Task 6 Evaluate siRNA for TREM-2 and DAP12 for inhibition of TNF production by THP-1 cells (Jessica Hamerman, PhD).

Task 6 is a component of Aim 1D. While Aims 1B and 1C target the adaptive immune response through control of Treg maturation and function, Aim 1D evaluates innate immune regulators as potential targets for anti-inflammatory intervention during wound repair. Specifically, Aim 1D assesses several endogenous inhibitors of the macrophage inflammatory response, TREM-2, BCAP, and β2 integrins, with the goal of developing strategies to down-modulate the macrophage inflammatory response as one of the multi-faceted approaches for cytoprotection examined in this project.

The macrophage inflammatory response is potently activated by pattern recognition receptors that include the TLR family, which, when ligated, results in the secretion of pro-inflammatory cytokines, such as tumor necrosis factor, IL-12, and IL-6, as well as chemokines that attract other immune cells. One mechanism by which the inflammatory response is controlled is through endogenous inhibitors or negative regulators of TLR signaling. In Aim 1D, we propose to investigate several inhibitors of TLR signaling, with the long-term goal to develop strategies for turning on these inhibitory pathways with either small molecules or soluble proteins that can be incorporated into the cytoprotective implant hydrogels to modulate the macrophage inflammatory response during wound repair.

We have spent several years investigating the anti-inflammatory receptor complex made up of the triggering receptor expressed on myeloid cells (TREM)-2 receptor and its dialkyl phosphate (DAP)12 signaling chain. Using mouse models, we have shown that TREM-2/DAP12 inhibits macrophage TLR responses both *in vitro* and *in vivo*. Accordingly, for the initial part of this project (Task 6), we investigated whether TREM-2 and DAP12 might serve as innate immune regulators by dampening inflammatory responses in human macrophages. To accomplish this, we performed experiments to knock down TREM-2 and DAP12 in human monocytes and monocyte-derived macrophages, using a set of corresponding siRNAs that targeted human TREM-2 and DAP12. We began our experiments by testing the effectiveness of the siRNAs in THP-1 cells, a monocyte-like cell line; however, we encountered difficulty in measuring the efficacy of knockdown when we
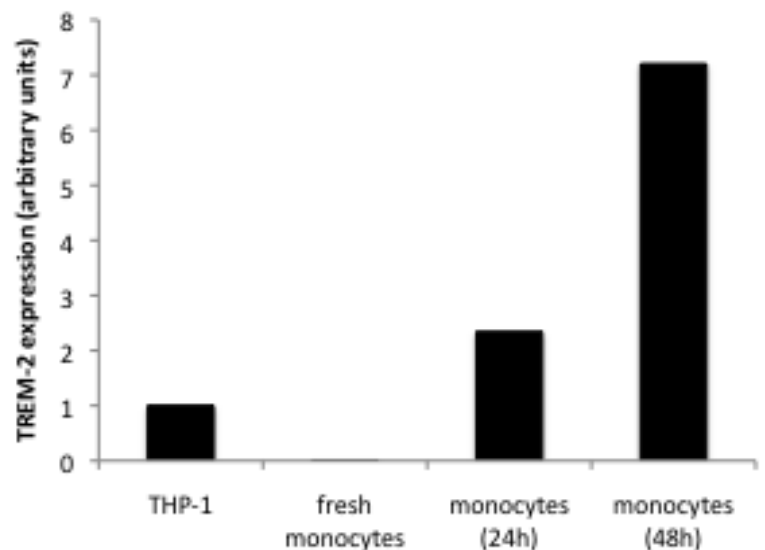

Figure 1. Expression of TREM-2 mRNA in THP-1 cells and CD14+ monocytes. CD14+ monocytes were isolated from PBMCs and either lysed for RNA or plated for 24 or 48 hours to induce expression of TREM-2 and then lysed for RNA. cDNA from these monocytes, or from THP-1 cells, were subjected to qPCR analysis for TREM-2.

used a flow cytometry-based method to detect of TREM-2 and DAP12 protein. As an alternative approach, we established a qPCR assay for measuring TREM-2 and DAP12 mRNA. **Figure 1** shows that we can measure TREM-2 mRNA in THP-1 cells and in cultured monocytes. We have not been successful in finding an antibody that recognizes TREM-2 for flow cytometry analysis; however, now that we have assays to measure DAP12 and TREM-2 mRNA, we plan to complete the testing of the different siRNAs for TREM-2 and DAP12 in THP-1 cells in Year 2.

Task 7 Measure TLR activation by cytokine production and phospho-specific antibodies in CD18 and BCAP KO mice, and map BCAP domains as potential therapeutic targets (Jessica Hamerman, PhD).

For Aim 1D, Parts 2 and 3, we investigated two novel inhibitors of TLR signaling, β2 integrins, and BCAP, using knockout mice. We began experiments in Quarter 2 to analyze TLR responses in CD18 (β2 integrin)-deficient mice. Wild-type or CD18-deficient mice were injected with 100 μg LPS and sera collected at 1, 2, 4, and 6 hours after injection. The amount of TNF, IL-6, and IL-12 p40 in the sera was then measured by ELISA. As shown in **Figure 1**, CD18-deficient mice produced more TNF and IL-12 p40 than wild-type mice, though the kinetics of induction was identical between wild-type and CD18-deficient mice. These data showed that CD18 inhibits TLR responses *in vivo* as well as *in vitro* in macrophages.
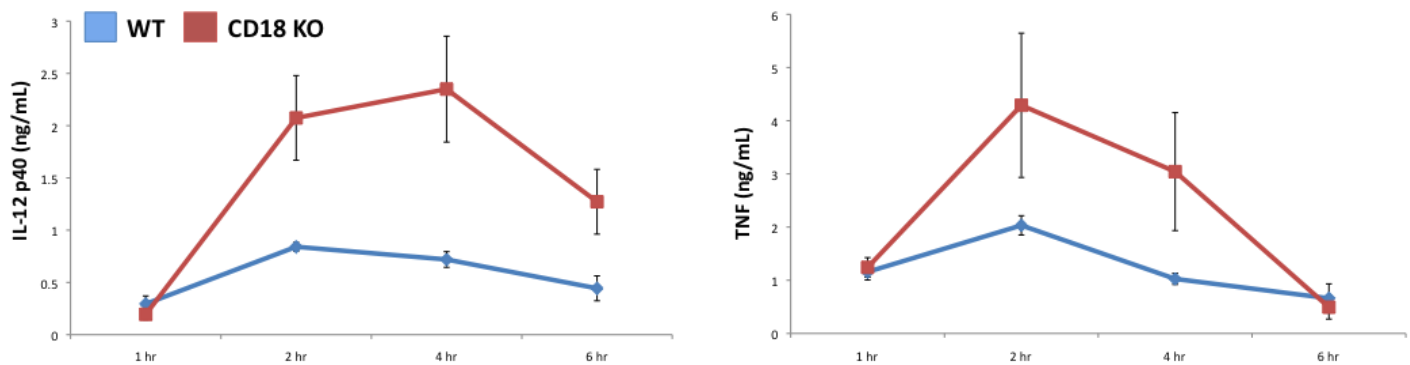
Figure 1. CD18 inhibits TLR responses in vivo. *Wild-type and CD18-deficient mice were injected with 100 μg of LPS. Sera were collected at 1, 2, 4, and 6 hours after injection. Serum cytokine amounts were measured by ELISA. Wild-type mice (WT) are shown in blue and CD18-deficient mice (CD18 KO) in red. Data are shown as mean +/- SEM. N = 5 mice per group.*

In Quarter 3, we compared cytokine production on a per cell basis from peritoneal macrophages from wild-type and CD18-deficient mice. We found that peritoneal macrophages from CD18-deficient mice produced more IL-6 and IL-12 p40 than those from wild-type mice, whereas the production of TNF was similar between the two genotypes (**Figure 2**). These data are similar to our findings with bone marrow-derived macrophages and further strengthen our conclusion that β2 integrins inhibit TLR signaling in a variety of macrophage populations.

13
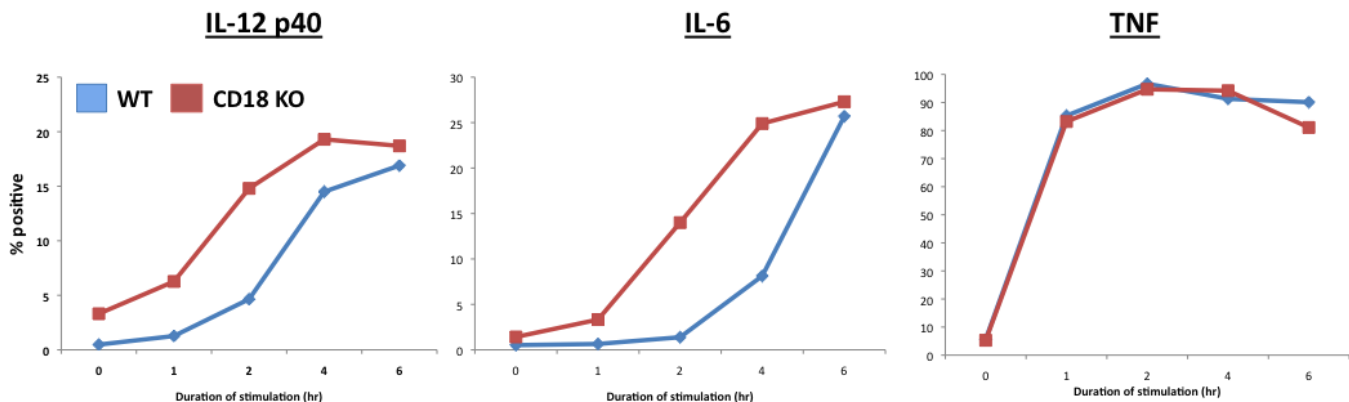
Figure 2. CD18-deficient peritoneal macrophages hyper-respond to TLR agonists. Macrophages were isolated from the peritoneal cavity of WT and CD18-deficient mice 3 days after injection of thioglycollate broth. The cells were cultured overnight and then treated with LPS for the indicated times, with Brefeldin A added for the last 4 hours. After harvest, cells were surface stained for F4/80 to identify macrophages, stained intracellularly for IL-12 p40, IL-6, and TNF, and analyzed by flow cytometry. The data are represented as the percent of F4/80 macrophages producing each cytokine.
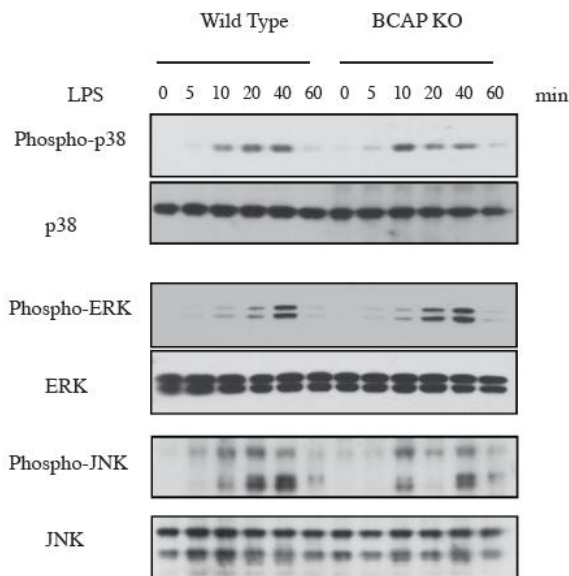
Figure 3. BCAP-deficient macrophages have slightly increased MAPK activation. WT or BCAP-deficient bone marrow-derived macrophages were treated for the indicated amount of time with 1 ng/ml LPS after which the cells were lysed and cytoplasmic extracts were generated. Cytoplasmic extracts were separated by SDS-PAGE and Western blotted with antibodies specific for different MAPK proteins or their phosphorylated forms.
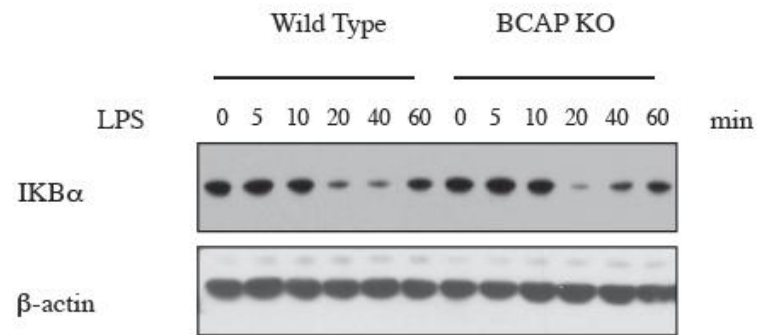
Figure 4. BCAP-deficient macrophages have no change in IκBα degradation. WT or BCAP-deficient bone marrow-derived macrophages were treated for the indicated amount of time with 1 ng/ml LPS after which the cells were lysed and cytoplasmic extracts were generated. Cytoplasmic extracts were separated by SDS-PAGE and Western blotted with antibodies specific for IκBα or β-actin as a loading control.

In Quarter 4, we expanded our studies beyond the inhibition of TLR responses by β2 integrins to investigate how BCAP inhibits TLR responses. This was done by comparing TLR-induced signal transduction in wild-type and BCAP-deficient macrophages. We treated wild-type and BCAP-deficient macrophages with LPS and prepared cytoplasmic extracts at different times after treatment. We then used SDS-PAGE and Western blot to examine the activation of the 3 MAPK signaling pathways and the activation of the NF-κB pathway. As shown in **Figure 3**, there was a slight enhancement of p38 MAPK and ERK phosphorylation after LPS treatment in BCAP-deficient macrophages in comparison with wild-type macrophages. In contrast, there was no change in the degradation of IκBα protein, the cytoplasmic inhibitor of NF-κB translocation to the nucleus (**Figure 4**). This leads us to conclude that BCAP-deficiency subtly affects the activation of MAPK pathways, but does not affect NF-κB activation. In Quarter 1 of Year 2, we will investigate how BCAP deficiency affects activation of the PI3-kinase pathway downstream of LPS.

Task 8 Measure serum biomarkers in 20 human subjects treated with IL1RA after inflammatory stimulus (Srinath Sanda, MD).

This Task is a component of Aim 1E. Cytokines mediate tissue injury and cellular dysfunction across a broad range of diseases. Specific cytokines, such as IL-6, are emerging as important mediators in sepsis and as prognostic indicators of systemic inflammation in patients with traumatic injury. Our conceptual understanding of wound healing has evolved to include a complex interaction of inflammatory cytokines. Over the past decade, numerous agents have been developed to block the action of specific cytokines. These therapies have revolutionized the treatment of autoimmune conditions, such rheumatoid arthritis and inflammatory bowel

disease. However, given the broad range of inflammatory mediated diseases, cytokine-modulating agents may have utility in other areas of medicine, as has recently been observed with the beneficial effect of the administration of TGF-β3 in wound healing.

Aim 1E tests the protective role of inflammatory cytokine blockade in humans prior to an inflammatory stimulus. Task 8 activated in Quarter 2, and that quarter was spent establishing a human subjects protocol, receiving local regulatory board approval, passing through a rigorous external scientific review, and receiving approval from the USAMRAA, the Office of Research Protections (ORP), and the Human Research Protection Office (HRPO).

In Quarter 3, we began to test the protective role of inflammatory cytokine blockade in humans prior to an inflammatory stimulus (induced hyperglycemia). As a consequence of our human subjects review process in Quarter 2, we made certain changes to our protocol, which included studying a total of 10 patients and use of a 3-day course of anti-cytokine blockade after the first study visit and prior to repeating the induced hyperglycemia. Thus far, we have enrolled a total of 5 patients in our study, who have completed both study visits. We have mechanistic data on the first 3 patients. Each patient presented to the clinical research center (CRC) and received an octreotide infusion to temporarily halt endogenous insulin secretion. They received a
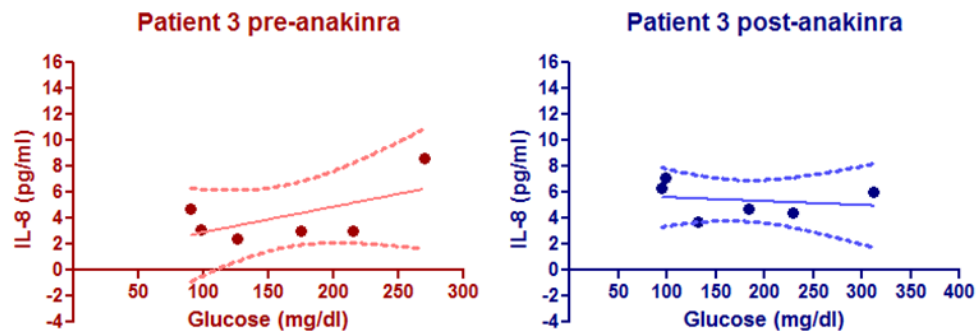
Figure 1. (Left graph) Glucose values on the X-axis and corresponding IL-8 levels. Note the overall trend for increasing IL-8 levels with increasing glucose. **(Right graph)** The same patient undergoing induced hyperglycemia but after receiving 3 daily doses of anakinra. Note the blunted IL-8 response.
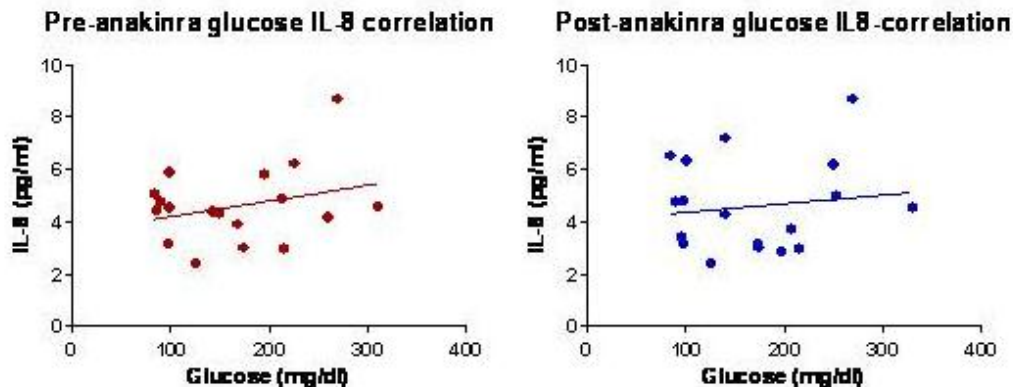
Figure 2. (Left graph) Glucose values on the X-axis and corresponding IL-8 levels. Note the overall trend for increasing IL-8 levels with increasing glucose. **(Right graph)** The same group undergoing induced hyperglycemia but after receiving 3 daily doses of anakinra. Note the blunted IL-8 response.

bolus of IV glucose and had sera and PBMCs collected for the next two hours. The subjects then received a daily dose of an IL-1 receptor antagonist, *anakinra*, for 3 days and returned to the CRC for a repeat of the octreotide/glucose combination. No significant adverse events occurred. Our major focus was the measurement of serum IL-8, a major inflammatory cytokine that is easily and reliably measured in sera after induced hyperglycemia. Although our initial numbers were too small to be statistically significant, the data set appeared

to show a positive effect with IL-1 blockade. As shown in **Figure 1 (left graph)**, there was a trend for increasing serum IL-8 levels after hyperglycemiwas induced at the pre-anakinra visit. However, after anakinra exposure (**Figure 1, right graph**), there did not appear to be the same rise in serum IL-8 levels despite comparable hyperglycemia, which suggested that we were blocking the generation of this inflammatory cytokine. Additional data points have been gathered from our first 3 patients (**Figure 2**), which support the initial trend of a blunted IL-8 response after administration of anakinra. We will continue to recruit and anticipate beginning cellular phenotyping of frozen PBMCs in Quarter 1 of Year 2. In particular, we will begin looking at IL-8 receptors and CD11b integrin expression on monocytes, as we have shown that these markers are sensitive to surrounding IL-8 levels.

<u>Task 9</u> **Production of the three-layer CI "sandwich" (Robert Vernon, PhD).**

Task 9 is a component of Aim 2A which involves the design and fabrication of the cyotprotective implant (CI). The CI will incorporate a number of novel features to optimize its functional properties: (1) a thin, flat, flexible shape that will conform to the varied dimensions of wound beds and graft sites; (2) a composition of ECM components that are nontoxic and biodegradable; and (3) inclusion of bioactive molecules selected for immune modulation, stimulation of angiogenesis, cell differentiation, and tissue regeneration. These bioactive molecules will be bound to the CI's ECM and will be released over time as the ECM biodegrades *in vivo*. A proposed form for the CI is a three-layered sandwich

Figure 1. Concept for the CI. A. Surface of the CI shows one of the gelatin sponges (GS, yellow), which is perforated with an array of holes (H), each 0.4 – 0.5 mm in diameter and filled with HMW-HA gel (pink). B. A cross-section through the CI (dotted line in A) shows the top and bottom gelatin sponges (yellow) and the central HMW-HA layer (HA-pink).

consisting of a crosslinked HMW-HA hydrogel compressed between two gelatin sponges (**Figure 1**).
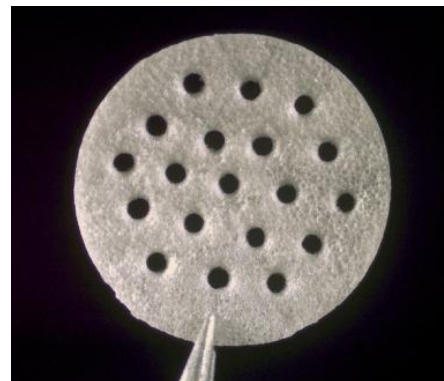
In Quarter 1, initial experiments focused on material selection for the CI. For the gelatin scaffold component, we produced prototype 0.75 mm – 1 mm thick gelatin sponges made by casting 10% bovine gelatin in a mold, followed by crosslinking with glutaraldehyde (GA) and freeze-drying. We also produced gelatin sponges crosslinked with 1-ethyl-3-(3-dimethylaminopropyl)-carbodiimide/N-hydroxysuccinimide (EDC/NHS), which is significantly less cytotoxic than GA and yields sponges with

Figure 2. Example of a 0.75 mm thick, 8 mm diameter, disk-shaped gelatin sponge prototype perforated with an array of 0.4 mm diameter holes. The gelatin in this prototype was crosslinked with EDC/NHS.

similar strength. The EDC/NHS crosslinked gelatin sponges were easily cut into a variety of shapes and could be perforated with 0.4 mm diameter holes (**Figure 2**). The sponges rehydrated readily, absorbing 85$^+$% water by weight. In addition to our own gelatin sponge constructs, we have evaluated a commercially available crosslinked gelatin sponge product (Gelita-Spon™, Invotec International, Jacksonville, FL) (**Figure 3**). This product is approved for clinical use, with a degradation rate of up to 4 weeks. It may be possible to reduce the rate of degradation by additional crosslinking with EDC/NHS.

In Quarter 2, we began studies to develop approaches for controlled release of cytokines within the CI. We determined that the HMW-HA hydrogel incorporating crosslinked heparin (Extracel-HP) could bind and release heparin-binding immunomodulatory growth factors, such as IL-2 and IL-10 (Task 3). In addition to this depot for storage and release of growth factors, we evaluated controlled release from calcium-crosslinked alginate hydrogel (in the form of 2 mm diameter "macrospheres") as a

Figure 3. Sample block of Gelita-Spon™ gelatin sponge (unhydrated).

16

way to deliver bioactive agents over extended time periods. We evaluated alginate by itself and also alginate that incorporated heparin-Sepharose microbeads (**Figure 4**). Incorporation of heparin microbeads substantially increased the growth factor-binding capacity of the alginate.


Figure 4. Alginate macrospheres of 2 mm diameter. The sphere on the left is comprised of Ca⁺⁺-crosslinked alginate only. On the right, a similar alginate sphere is filled with heparin-Sepharose microbeads with an average diameter of 90 microns.
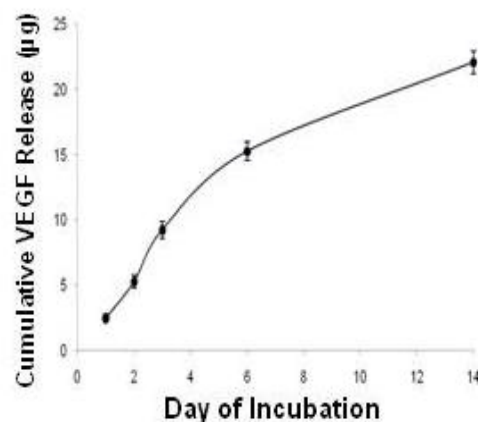
Figure 5. Controlled release of VEGF from alginate macrospheres. Alginate macrospheres of 2 mm diameter (without heparin-Sepharose microbeads, similar to the one shown on the left side of Figure 4) were loaded with 50 ng of VEGF and incubated in culture medium in vitro under physiological conditions for two weeks. During this time, the release of VEGF into the culture medium was assessed at specific time points. Over the 2-week period, approximately half of the VEGF was released. Release kinetics was bilinear, with a steeper release in the first week followed by a shallower release in the second week.

Significantly, we were able to show that alginate macrospheres loaded with the angiogenic cytokine vascular endothelial growth factor (VEGF) could release this molecule in a controlled fashion over a period of at least 2 weeks (**Figure 5**). VEGF will likely prove to be an important component of the CI for its capacity to induce vascular growth within wound sites and at the sites of regenerative tissue grafts.
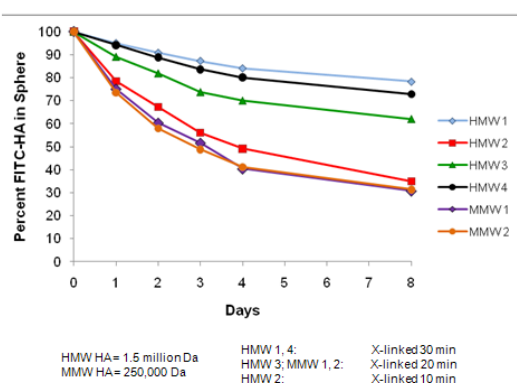

Figure 6. Controlled release of compounds from alginate is influenced by the degree of crosslinking. Alginate macrospheres containing fluorescent (FITC)-labeled HMW-HA were monitored for HA release over 8 days. Alginate crosslinked with Ca⁺⁺ for increasing lengths of time released the HA at a slower rate. HA of lower middle molecular weight (MMW) was released more rapidly than HMW-HA.
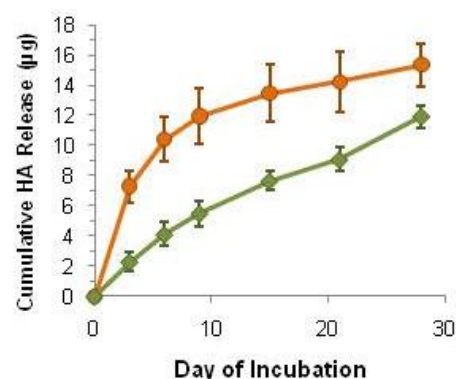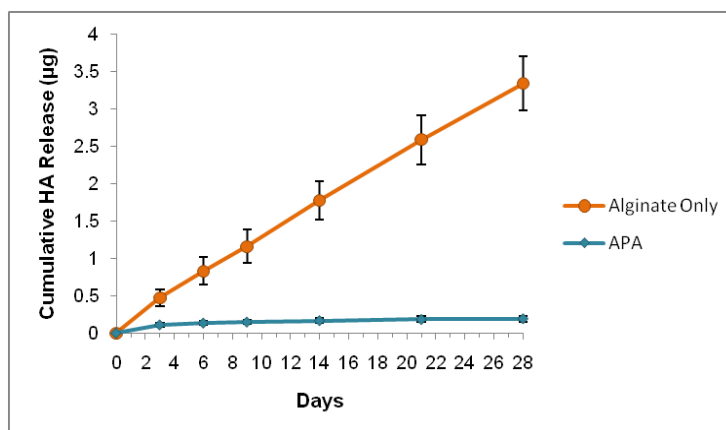

Figure 7. Controlled release of HMW-HA from alginate is prolonged and influenced by the degree of crosslinking. Alginate macrospheres (2 mm in diameter), each containing 32 µg of HMW-HA and 0.8 µg of fluorescent (FITC-conjugated) HMW-HA as a tracer, were monitored for HA release under physiological conditions in vitro over 28 days. Alginate crosslinked with Ca⁺⁺ for 30 min (green plot) released HMW-HA in a linear manner over the course of the study. Notably, only a third of the HA was released from this sphere set (n = 5) in 28 days, suggesting a potential for controlled release of up to 3 months.

A particularly exciting development is our finding that the alginate can be used as a controlled-release agent to deliver soluble HMW-HA. Our results

indicate that the rate of release of HMW-HA can be controlled by the length of time the alginate is crosslinked with Ca^{++} (**Figure 6**). Importantly, release of the HMW-HA can occur over a prolonged period of time (**Figure 7**). In light of our finding that HMW-HA stimulates regulatory T-cells (Task 3), the ability to deliver this molecule locally over a prolonged period via controlled release (using biocompatible alginate) may prove to be an effective means to control inflammation within wound and graft sites.
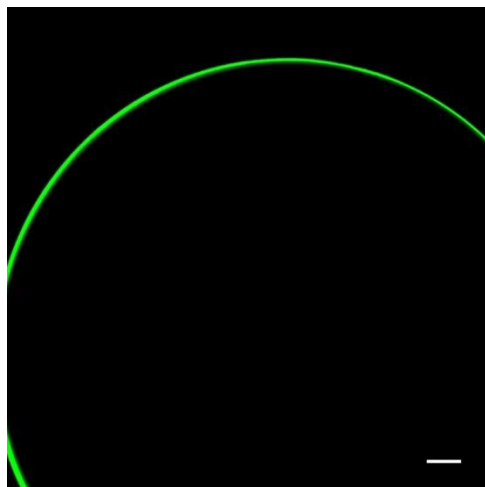
Figure 8. PLL-coated alginate macro sphere. An alginate macrosphere of 2 mm diameter was incubated for 1.5 h in 1 mg/ml of PLL and then stained with genepin to reveal the PLL bound to the alginate. In this confocal microscopic image, the PLL layer is seen as a thin, fluorescent green shell on the surface of the alginate. Scale bar = 100 microns.

Figure 9. Effect of PLL exposure on release of HMW-HA from alginate. Ca^{++}- crosslinked, 2 mm alginate macrospheres containing HMW-HA and fluorescent HMW-HA tracer were incubated for 1.5 h in 1 mg/ml of PLL or saline only and then were monitored for HA release under physiological conditions in vitro. The spheres lacking the PLL coat released HA in a linear fashion over 28 days (orange plot), whereas the spheres coated with PLL did not release HA (blue plot). n = 5 for both sphere sets.

In addition to development of alginate-mediated, controlled release of HMW-HA, we explored methods to use alginate matrices to deliver immunomodulatory compounds of lower molecular weights. For these studies, we used alginate spheres coated with poly-L-lysine (PLL) (**Figure 8**). Addition of a PLL coating to alginate spheres creates an outer "shell" of high density positive charge on the sphere, which has the potential to slow the diffusion of bioactive compounds from the interior of the sphere and serve as a depot of positive charges to retain negatively charged immunomodulatory compounds, such as IL-10 and TGF-β. We first evaluated the effect of alginate on release of HMW-HA. We found that incubation of alginate spheres in a solution of 1 mg/ml of PLL for 1.5 hours completely blocked the release of HMW-HA over 28 days (**Figure 9**). In experiments currently underway (data not shown), we are finding that exposure of the alginate spheres to lower concentrations of PLL permit release of HMW-HA, but at a slower rate than spheres not exposed to PLL, suggesting that PLL may be an effective means of regulating HMW-HA release as an alternative to regulation via Ca^{++} crosslinking. In Quarter 1 of Year 2, we will evaluate the capacity of PLL-coated alginate spheres to bind and release IL-10, TGF-β, and antibodies (such as anti-CD3 and CD28) in a controlled manner.

Task 10 Evaluation of prototype CI in rat dermal pockets for histological monitoring of biodegradation and in mouse dermal pockets for evaluation of regulatory T cell responses (Robert Vernon, PhD).

In our first set of studies, we observed that the Gelita-Spon™ gelatin sponge was degraded *in vivo* within 3-4 days. In addition, we evaluated the degradation properties of implanted Extracel-HP hydrogels after 7 days of residence in the peritoneal cavity of mice (in contact with gut mesentery). By histology (**Figure 1**), we found evidence of a measured degradation of the HMW-HA hydrogel by macrophage-like "giant cells," associated with a fibrovascular cellular infiltrate (**Figure 1A**). This degradation was accompanied by vascularization of the site (**Figure 1B**). The process of degradation was accelerated by reducing the degree of thiol crosslinking of the hydrogel (**Figure 1C**).

We have demonstrated that our HMW-HA hydrogels can bind and release IL-2 and IL-10 (Task 3), and we have shown that soluble HMW-HA can be released in a controlled manner from calcium-crosslinked alginate (Task 9). In Year 2, we will incorporate these immunomodulatory agents into prototype CIs and evaluate their effects on post-implantation foreign body responses to the CIs. We evaluated allo-immune responses to implanted, cytokine-loaded, crosslinked HMW-HA hydrogels (Extracel-HP) CIs. These allo-responses were induced by incorporating Balb/c-strain mouse cell lysates into the CIs and implanting them into B6-strain mice. Our preliminary findings (by histology) suggested that there may be a protective effect on engrafted (islet) tissue; however, these experiments must be repeated to determine if the observations are valid.
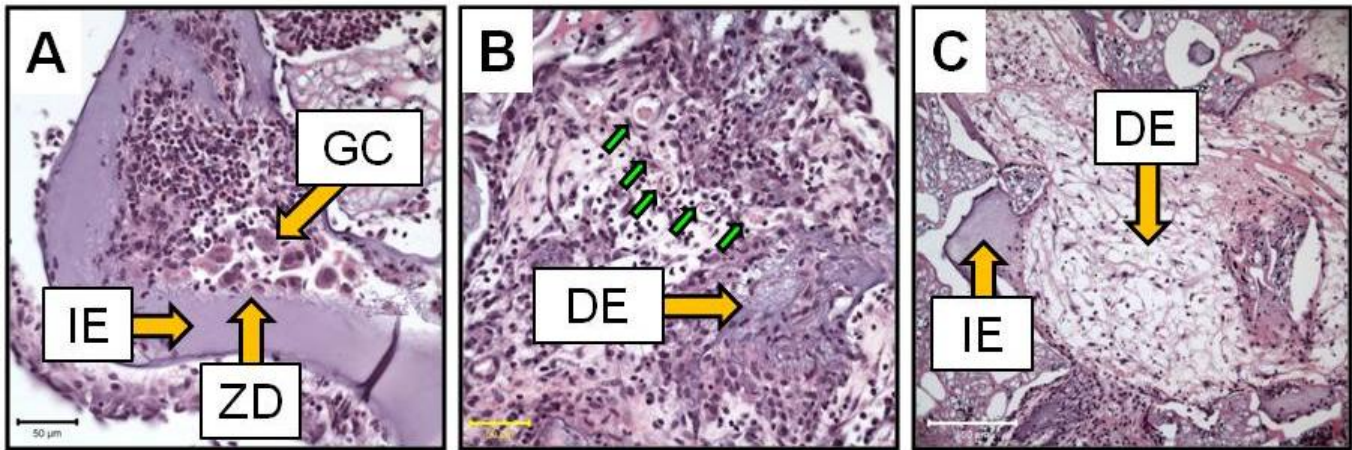
Figure 1. Cellular response to Extracel-HP 7 days after implantation in the mouse peritoneal cavity. *Micrographs are of paraffin sections cut at 8 microns and stained with hematoxylin and eosin.* ***A.*** *Areas of intact Extracel (IE) show uniform basophilia and do not contain cells. Cellular infiltrate contains giant cells (GC) that make contact with the Extracel matrix in a "zone of degradation" (ZD) where the Extracel is broken down.* ***B.*** *Where the implant has become colonized by cellular infiltrate, degraded Extracel (DE) is observed in association with neovasculature (green arrows).* ***C.*** *An implant containing Extracel, with half the amount of thiol crosslinking than was done for the implant shown in Panels A and B, is cellularized more rapidly. Areas of intact Extracel (IE) and cellularized, degraded Extracel (DE) are shown.*

In Year 2, we will also evaluate the effect of controlled release of soluble HMW-HA from alginate macrospheres (Task 9). Our studies thus far indicate that, after implantation *in vivo*, the alginate of the macrospheres is not immunogenic, does not support infiltration by cells, and does not biodegrade, at least over the short term (**Figure 2**); therefore, the release kinetics of HMW-HA from alginate that we observe *in vitro* (Task 9, Figures 6, 7, and 9) may be similar after the macrospheres are implanted *in vivo*. Also of note, our initial experiments that evaluated controlled delivery of VEGF in mice indicated that incorporation of VEGF into alginate macrospheres induced an angiogenic response after implantation.
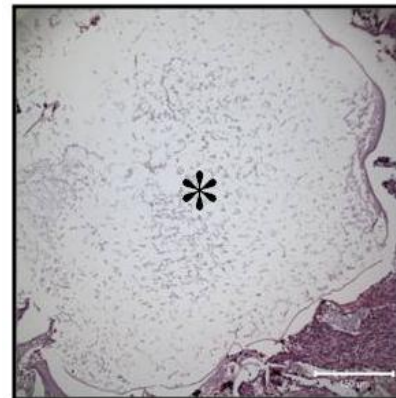
Figure 2. A 2 mm diameter alginate macrosphere 7 days after implantation in the mouse peritoneal cavity. *Micrograph is of a paraffin section cut at 8 microns and stained with hematoxylin and eosin. The macrosphere (asterisk) is largely intact. The alginate appears as a precipitate–a consequence of removal of water from this highly-hydrated hydrogel during histological processing.*

Task 11 Development of myobridges using uniaxial supports and collagen gels populated with myoblastic cells. Histological evaluation of cultured myobridges for cell survival, new muscle cell generation, proliferation and differentiation (Margaret Allen, MD, Robert Vernon, PhD).

Developing fabrication techniques for myobridge constructs

In Quarter 1, as an autologous cell source for myobridges, we selected muscle-derived stem cells (MDSCs). In humans, these cells can be procured from skeletal muscle biopsies and expanded ex vivo, and, after implantation, they have been shown to reliably differentiate into myotubes and skeletal muscle. Over several years, we have perfected existing techniques to isolate MDSCs from both mouse and rat skeletal muscle. This project utilizes rat MDSCs to generate constructs that can later be implanted into the larger muscle defects created in rats vs. mice, to provide a rigorous test of muscle-regenerative potential.

A goal of Task 11, a component of Aim 2B, is to develop myobridges that would be suitable for later *in vivo* implantation, with an eye to providing a milieu for implanted myoblastic cells that will foster cell survival and proliferation while reducing ambient host inflammation. We have previously shown that upregulation of heme oxygenase-1 (HO-1) by a specific transcriptional activator, cobalt protoporphyrin (CoPP), increases the percentage of MDSCs that survive an *in vitro* regimen of hypoxia/ reoxygenation, designed to mimic the stresses of *in vivo* cell implantation. Our initial experiments in Quarter 1 explored whether CoPP might be an appropriate additive to construct scaffolds.

Type I collagen gels with CoPP

In our initial pilots, rat MDSCs were seeded into 100% collagen gels that were then suspended on Nitex nylon mesh frames and cultured for 5 days. Groups of construct scaffolds (*n* = 2 scaffolds per group) differed in CoPP treatment and delivery route: (1) control type I collagen gels without additives; (2) 25 µM CoPP added to the culture differentiation medium (DM) 24 hours after cell seeding; (3) 25 µM CoPP added to the scaffold upon seeding; (4) 25 µM CoPP added to the scaffold upon seeding plus CoPP added to the medium at 24 hours after seeding. At the end of the 5-day culture, constructs were collected and formalin fixed.
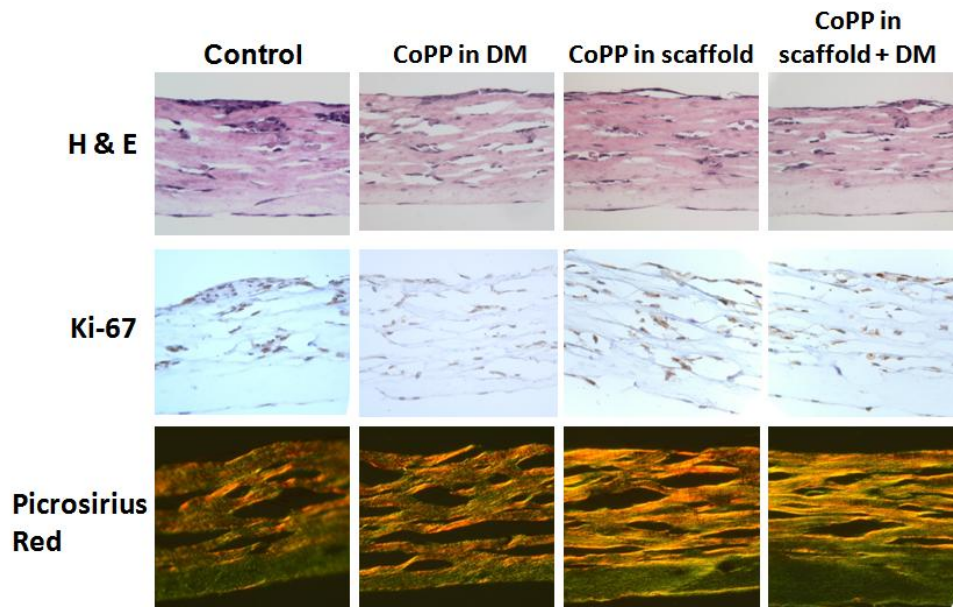
Figure 1. Histology results from rat MDSCs seeded into collagen gels treated with CoPP.

The results (**Figure 1**) suggested that adding CoPP increased the numbers of surviving cells, especially those deep within the constructs. CoPP treatment also appeared to increase MDSC proliferation within the scaffolds, visualized as more cells exhibiting Ki-67 staining (indicative of dividing cells) in all CoPP-treated specimens.

Finally, more picrosirius red staining was seen in the groups in which CoPP had been incorporated into scaffolds, suggesting that the capacity for MDSCs to reorganize collagen was enhanced in CoPP-treated scaffolds.

*Combined collagen/hyaluronan gels with CoPP*

In the set of experiments started in Quarter 2 (**Table I**), CoPP was added to two candidate scaffold materials for myobridge fabrication: 100% collagen and a mixture of 95% type 1 collagen with 5% Hystem-HP™. HyStem-HP™ (Glycosan Biosystems) is an extracellular matrix hydrogel that contains cross-linked HMW-HA, which has been used to advantage in the growth of other stem cell types, but has not been previously used with skeletal myocytes. HMW-HA is expected to have anti-inflammatory properties and the cross-linking is designed to prevent breakdown into pro-inflammatory low molecular weight fragments. Heparin immobilized within the Hystem-HP™ would allow for slow release of growth factors (GFs). In addition, Hystem-HP™ should alter the stiffness of the construct, which may make it easier to handle and implant surgically.

MDSCs were seeded into 100% collagen or 95% collagen/5% Hystem-HP™ constructs with and without the addition of 25 µM CoPP to the scaffold. Constructs were seeded at cell densities of 2.2 x 10^6 cells/ml, or 10^6 cells in 450 µl matrix per construct. We used rat serum to better simulate the milieu surrounding the construct after *in vivo* implantation in rats. After 24 hrs, the collagen constructs were incised laterally to instill tension and transferred to differentiation medium for *in vitro* status for 2 or 3 weeks.

Table I. Experimental design: constructs seeded with rat MDSCs cultured in vitro.

		Fixed in 10% buffered formalin	
	Initial Number	14 days	21 days
TREATMENT GROUPS			
100% collagen	4 constructs	2 constructs	2 constructs
100% collagen + CoPP	4 constructs	2 constructs	2 constructs
95% collagen/5% HystemHP	4 constructs	2 constructs	2 constructs
95% collagen/5% HystemHP + CoPP	4 constructs	2 constructs	2 constructs

* MDSCs suspended at 2.22x10^6/ ml of matrix material (100,000 cells in 450 µl of matrix per construct).
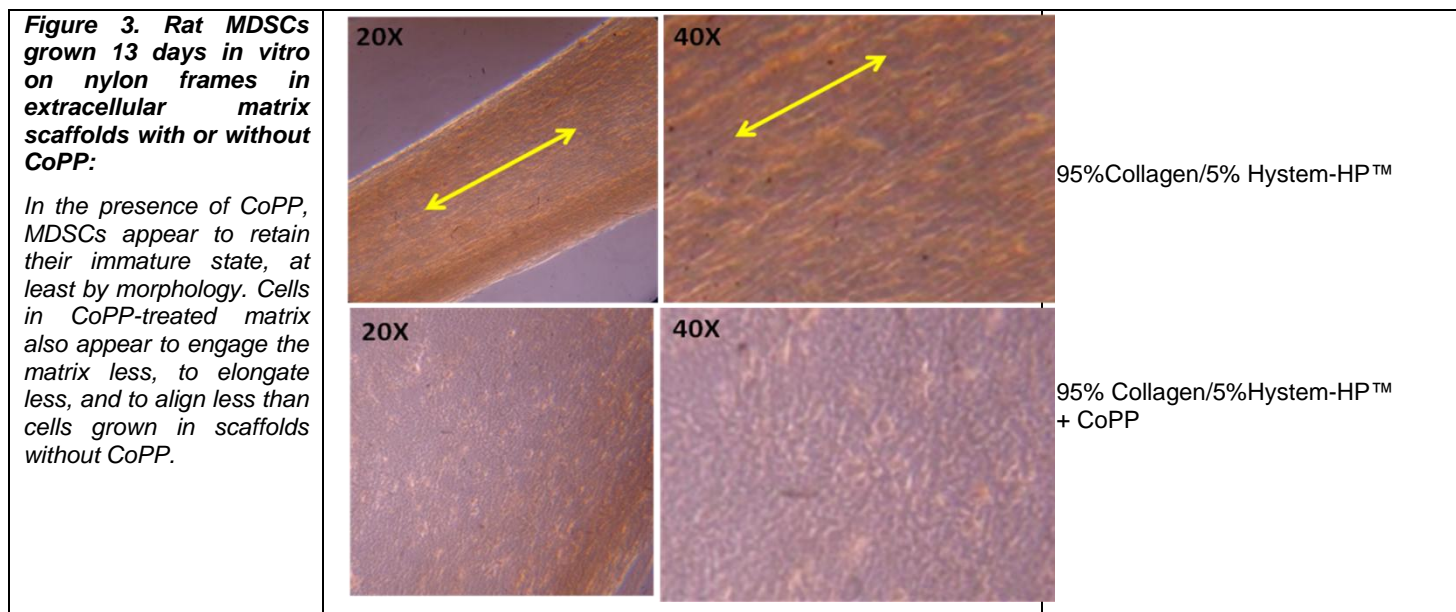
13 days in constructs, 20X
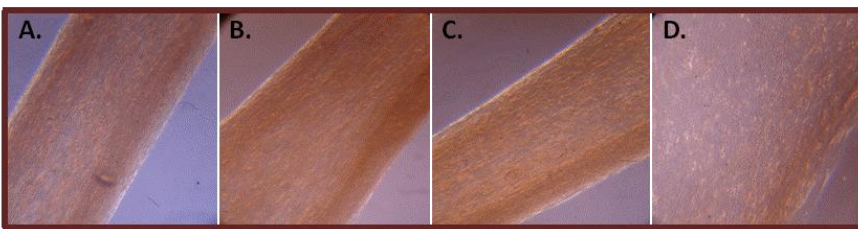
21 days in constructs, 20X
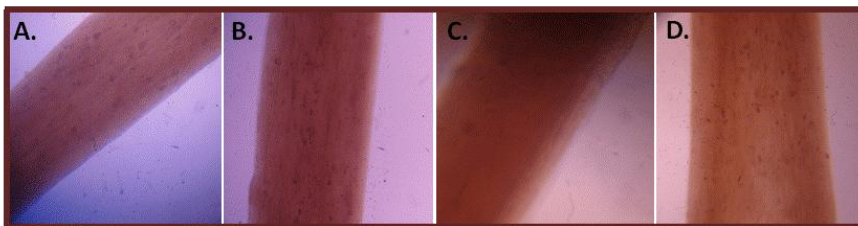

Figure 2. Rat anterior tibialis MDSCs grown in vitro on nylon frames in extracellular matrix scaffolds with or without CoPP:

A.   100% collagen

B.   100% collagen + 25 µM CoPP

C.   95% collagen/5% Hystem-HP™

D.   95% collagen/5% Hystem-HP™ + 25 µM CoPP.

21

Figure 3. Rat MDSCs grown 13 days in vitro on nylon frames in extracellular matrix scaffolds with or without CoPP:

In the presence of CoPP, MDSCs appear to retain their immature state, at least by morphology. Cells in CoPP-treated matrix also appear to engage the matrix less, to elongate less, and to align less than cells grown in scaffolds without CoPP.

95%Collagen/5% Hystem-HP™

95% Collagen/5%Hystem-HP™ + CoPP

Histology results from these *in vitro* studies suggested that the addition of CoPP, to either the 100% collagen matrix or to the combined collagen/hyaluronan matrix, changes the appearance of the cells in the constructs, at least at the early 2-week time point (**Figures 2–4**). In the presence of CoPP, cells appeared rounder and less elongated, and exhibited less alignment during culture under uniaxial tension.
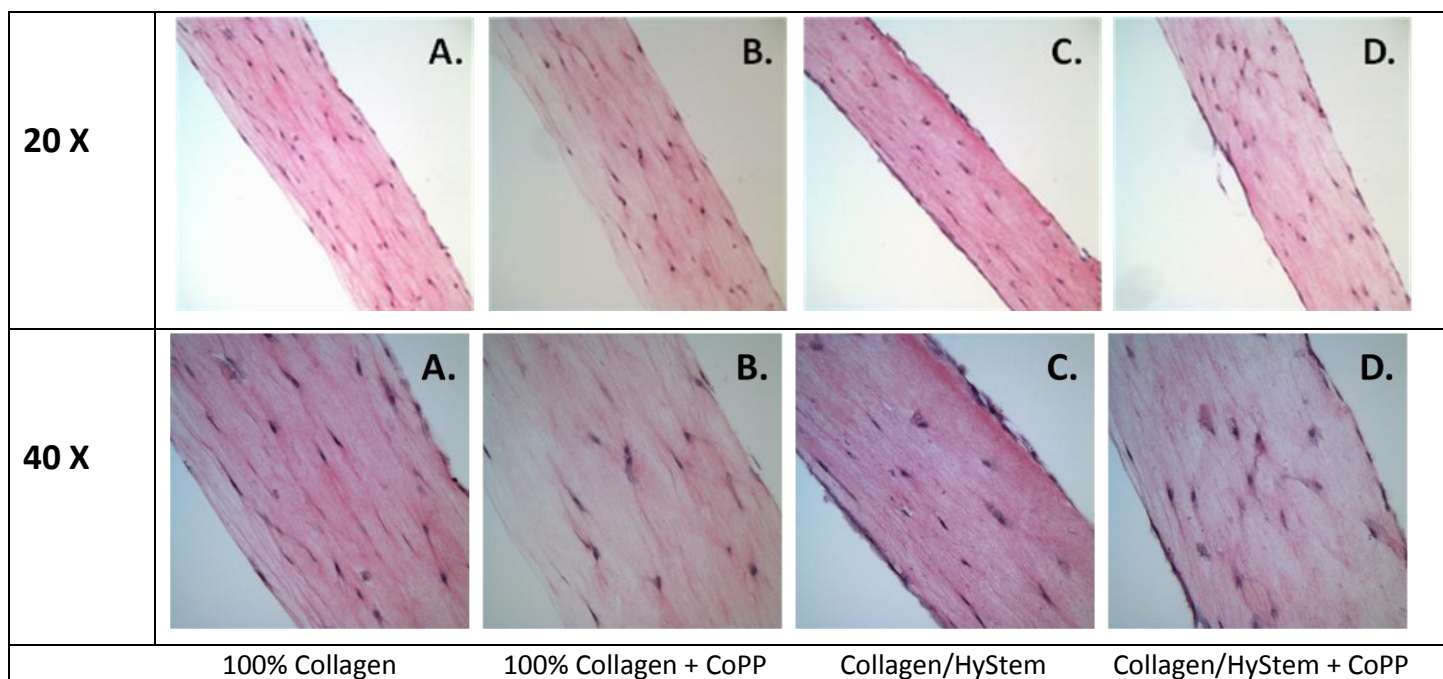
Figure 4. Hematoxylin and eosin staining of MDSC-seeded constructs at 13 days. *More cells seem to aggregate on the surface of scaffolds containing hyaluronan (Hystem-HP™) in comparison with pure collagen scaffolds. The cells grown in scaffolds with CoPP appear to be less elongated and less aligned than those grown in the absence of CoPP, but more specimens and immunostaining are needed to confirm this observation.*

Picrosirius Red staining (**Figure 5**) showed that the presence of CoPP in the scaffold appeared to be associated with smaller-sized collagen fibers in the construct. This again suggests that CoPP may be slowing down the differentiation process, so that less collagen remodeling is occurring with the addition of CoPP. Alternatively, CoPP could be altering cell adhesion to matrix or the strength of cell traction on the matrix. If,
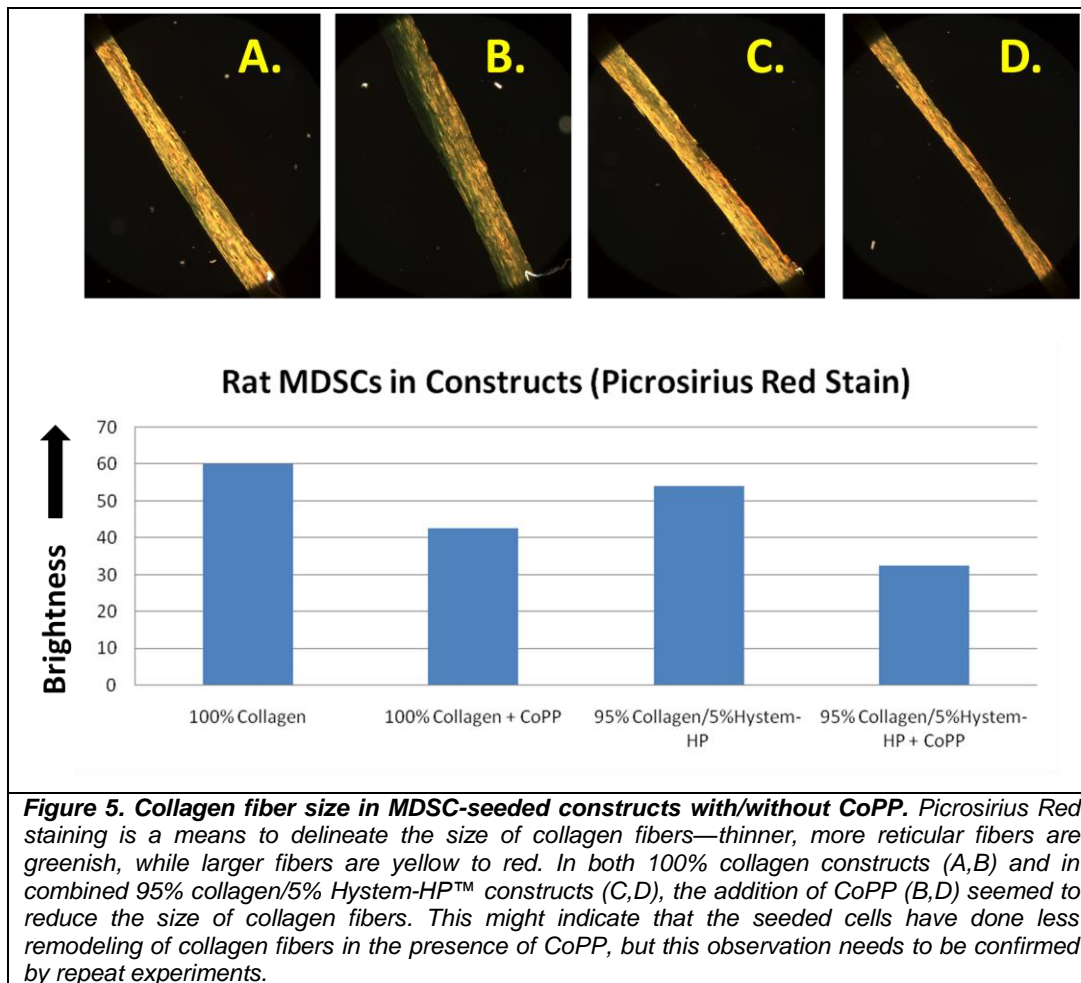
indeed, CoPP slows MDSC differentiation, this might be advantageous for myobridge implants, since MDSCs that stay in a more immature state may have greater proliferative potential after *in vivo* implantation. This might facilitate more complete replacement of lost muscle.

Finally, initial histology results suggested some difference in cell behavior in the hyaluronan matrices (**Figure 4**). Cells in the combined collagen/hyaluronan matrices appeared to be more densely situated on the surface of the construct than the cells grown in 100% collagen. Whether this reflects increased proliferation will be examined with Ki67 staining. The stiffness of the matrix may also affect the penetration of seeded cells. Glycosan Biosystems will be measuring the stiffness of various Hystem-HP™ concentrations, so that this can be controlled.

Scaling up the molds for myobridge constructs

In the *in vitro* studies conducted in Quarter 2, MDSC-seeded gels were suspended in small rectangular Nitex frames. However, more sophisticated constructs were necessary for the *in vivo* implants. The goal here was to develop a myobridge that supports MDSC growth and differentiation, but that is also "implant ready" for use in repairing rat hindlimb muscle defects in our rat model. "Implant ready" means that the construct would contain appropriate scaffold material infused with viable cells, and that the construct ends would be ready to be attached directly to both ends of the native muscle defect. In concept, the seeded cells would be precultured under tension, so that they would already be aligned at the time of implantation.

Figure 5. Collagen fiber size in MDSC-seeded constructs with/without CoPP. Picrosirius Red staining is a means to delineate the size of collagen fibers—thinner, more reticular fibers are greenish, while larger fibers are yellow to red. In both 100% collagen constructs (A,B) and in combined 95% collagen/5% Hystem-HP™ constructs (C,D), the addition of CoPP (B,D) seemed to reduce the size of collagen fibers. This might indicate that the seeded cells have done less remodeling of collagen fibers in the presence of CoPP, but this observation needs to be confirmed by repeat experiments.
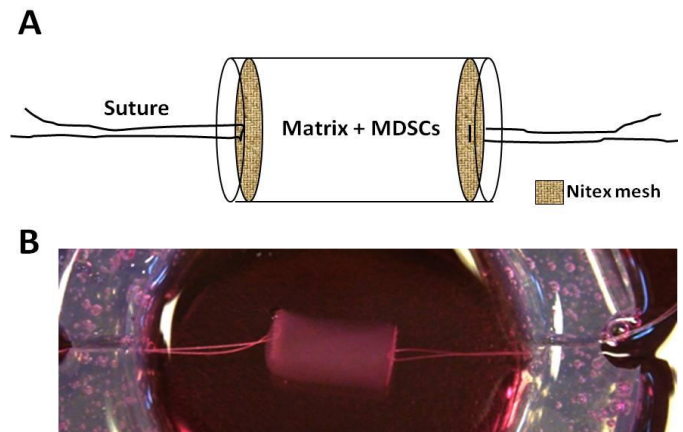
23

Several design problems needed to be solved for this concept to be realized: (1) the seeded cells actively and rapidly remodel the collagen scaffold, shrinking its diameter, so the initial mold should account for this and other geometric changes; (2) the collagen matrix needs to be firmly tethered at either end of the construct to maintain tension during the shrinkage process; this tension also needs to be maintained during implantation; and (3) the ends of the construct need to be suturable for easy surgical implantation. Ideally, the suture would also be biodegradable, so that the implant eventually consists solely of cells and natural scaffold without synthetic material.

To address each of these requirements, the following scaffold-suture construct was designed (**Figure 6A**). Each of the ends are composed of resorbable 6.0 vicryl sutures that are tied to discs of

Figure 6. Scaffold-suture construct design. *The design of the construct (A) includes sutures attached to Nitex meshes gelled within the matrix material containing MDSCs. An example of a fully polymerized collagen-based test construct is shown in B.*

Nitex mesh, which are then immersed in a collagen matrix solution and allowed to polymerize, thus encasing the Nitex mesh within the collagen hydrogel polymer (**Figure 6B**).
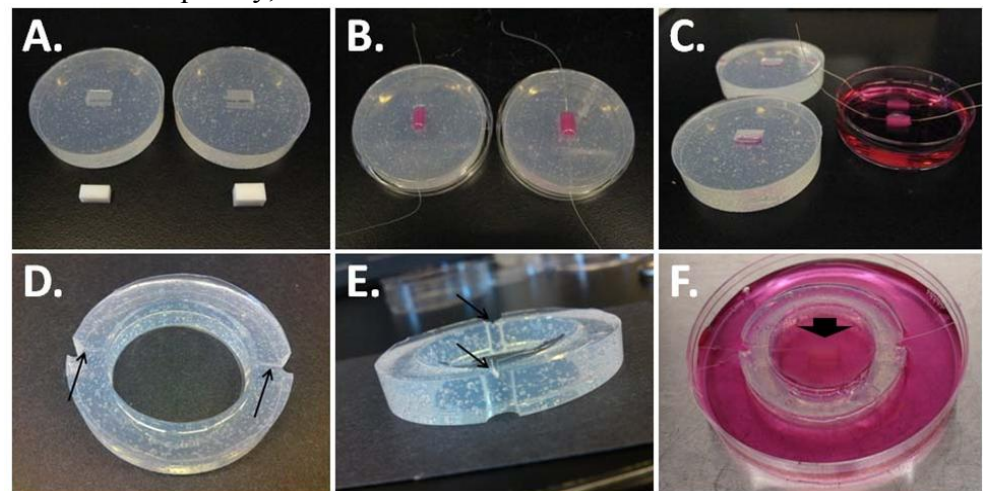
The entire fabrication process is illustrated in **Figure 7**. First, silicone "coffin molds" are fabricated by pouring a base layer of silicone and then pouring a second layer that contains Teflon blocks in whatever dimensions are desired. The Teflon blocks are then removed after the silicone has set up (**Figure 7A**), leaving a rectangular space (coffin) in the silicone. Subsequently, thin slits are cut into the silicone to connect with the two narrow walls of the coffin. These slits will secure both of the sutures, with their attached Nitex discs.

To prepare the scaffold-suture constructs, the suture/Nitex assemblies are placed within the sterilized mold into which is poured the extracellular matrix scaffold material with suspended cells. Collagen with MDSCs is the initial matrix/cell combination of choice, although other matrix and cell types will be tested. Subsequently, the filled mold is placed in a humid chamber at 37° C to polymerize the collagen (**Figure 7B**). After the collagen polymerizes, the entire construct is gently transferred into medium-filled culture plates (**Figure 7C**). To

Figure 7. Fabrication of scaffold-suture constructs using silicone molds. *"Coffin molds" are formed around Teflon blocks (A) and the suture/Nitex assemblies placed into the mold and the collagen/MDSC composite is allowed to polymerize around the Nitex material, tethering both ends (B). Once polymerized, the entire construct can be removed and placed into culture medium (C). To culture the constructs, a ring of silicone is formed (D and E) with two slits (arrows) to hold the suture ends in place. A complete culture setup within a 100 mm culture dish is shown in F, where the suture ends of the construct are tethered to the silicone ring with the construct (arrow) held in the center of the ring. The 100 mm culture dish is filled with enough culture medium (pink) to immerse the construct and then placed in a tissue culture incubator.*

culture the constructs *in vitro*, a silicone ring is formed by pouring silicone into a 60 mm dish that has a 35 mm dish in the center. After the silicone has solidified, two cuts are made, bisecting the ring with thin slots that will hold the construct sutures in place (**Figure 7D, E**). The sutures of the polymerized construct are inserted into

the slots of the silicone ring, which is then placed into a 100 mm culture dish (**Figure 7F**). The dish is filled with enough culture medium to immerse the construct and then placed in a tissue culture incubator.

During culture, the MDSC-collagen composite will contract, thus putting the entire construct under tension and orienting both the collagen fibrils and the seeded cells in parallel to the long axis of the construct. We have previously shown in our rectangular Nitex frames that this uniaxial tension results in the alignment of the myoblasts and myotubes along the line of tension. In Year 2, several geometries of the coffin molds will be tested, as we become familiar with how the constructs contract when combined with cells.

Although the current design has biodegradable sutures, the Nitex endplate material does not resorb. The current plan is to insert a new suture into the ends of the mature construct, which would have much greater strength by then, and then simply slip off the Nitex endplate material. However, another option for translating this setup to clinical applications would be to substitute some other resorbable material for the Nitex (e.g., a chitosan-alginate mesh). It can be seen that this technology could be readily developed into multiple parallel modules and extended to accommodate any length of construct.

It is expected that construct stiffness itself will contribute to the myogenic differentiation process, as has been illustrated in several recent publications [1-3]. We hypothesize that both cellular and matrix components will contribute to the overall construct stiffness, especially as cells multiply. One of the future directions, although perhaps beyond the scope of the current proof-of-principle proposal, will be to measure and adjust the tension on these constructs and determine whether there is a relationship with tensile strength, myogenesis, myotube and collagen alignment, and the ultimate strength of the fully differentiated implant.

Combined collagen/hyaluronan gels with HO-1 induction for cytoprotection

In preparation for upcoming Task 13 (supplementation of myobridges with CoPP and regulatory modulators) next year, we have begun development of scaffolds that include the heme oxygenase-1 (HO-1) inducer, cobalt protoporphyrin (CoPP) for use in the myobridges. Given the positive effects we have seen with this porphyrin in protecting both MDSCs and adult skeletal muscle from ischemia-reperfusion injury, we expect that slow release of CoPP in the scaffold should similarly promote the survival of seeded MDSCs *in vivo*. Moreover, data from our lab demonstrate an important additive effect of HO-1 induction on enhancing host vascularization of engineered cardiac tissue, so we are hopeful that CoPP will also accelerate host vascularization of skeletal muscle. Both the addition of CoPP and HMW-HA may have effects on maintaining MDSCs in a relatively dedifferentiated state.

Pilot in vivo implants

The initial *in vivo* pilot experiments listed below have been completed (**Table II**). These will serve as some of the controls for the upcoming series of implants in Task 12 (implantation of cell-seeded myobridges) to be conducted in Year 2.

Table II. Experimental design: treatment groups for in vivo implants conducted to date.

Pilot Study - Myobridge Implantation		Implant Procurement			
	Initial Number	Week 1	Week 2	Week 3	Week 4
Removal of AT Muscle	2 rats		1 rat		1 rat
Removal of AT Muscle replaced with Vicryl Suture	2 rats		1 rat		1 rat
Removal of AT Muscle replaced with 100% Hystem HP	4 rats	1 rat	1 rat	1 rat	1 rat
Removal of AT Muscle replaced with 100% rat type 1 collagen	4 rats	1 rat	1 rat	1 rat	1 rat
Removal of AT Muscle replaced with 100% Hystem HP with MDSCs	4 rats	1 rat	1 rat	1 rat	1 rat
Removal of AT Muscle replaced with 50% Hystem/50% collagen with MDSCs	4 rats	1 rat	1 rat	1 rat	1 rat
Removal of AT Muscle replaced with 100% rat type 1 collagen with MDSCs	4 rats	1 rat	1 rat	1 rat	1 rat
* MDSCs cells suspended at 2.22×10^6 /ml of matrix material					
** 300 µl of matrix implanted into cavity where AT muscle had occupied (66,700 MDSCs implanted)					

AT = anterior tibialis muscle

In the first group, the tibialis anterior muscle was simply excised, fixed, and measured to determine mold dimensions. Next, various suturing techniques were tested for securing Vicryl sutures to the anterior tibialis

tendon and muscle remnants to hone the implant techniques for these scaffold-on-a-suture constructs. Then, the first set of *in vivo* implants was performed, implanting just acellular scaffold materials alone without cells. These will serve as baseline studies to examine the extent and time course of native muscle regeneration and muscle cell repopulation of the scaffolds without cell implantation. Also, we will get an initial snapshot of the time course of leukocyte infiltration and host vascularization/angiogenesis of the different matrices, with and without the cytoprotective agent CoPP. This series will help us formulate which two time points will be used for larger experimental groups.

To date, the rat subjects have tolerated the implants well. They are able to walk on their operated legs and do not show signs of local inflammation. The Hystem HP scaffold was found to absorb water and increase in size after implantation, not seen in 100% collagen scaffolds, so this size change has been taken into consideration in calculating construct sizes. We also found that it is not practical to close the fascia over the implanted construct, but rather just the skin.

At the appropriate end point, the left hindlimbs were procured and fixed in 10% buffered formalin for a minimum of 5 days. The implant was then sectioned off the bone, leaving a margin of surrounding muscle, processed, embedded, and cut into tissue sections for histology. Upon sectioning, some of the construct tissues began to delaminate, likely due to the differences in composition and density between the soft gels and surrounding denser fascia and skin. This problem has been seen in other tissues (e.g., mouse ears) and was corrected by lengthening processing times. We plan to make several adjustments to our histology methods to optimize our tissue processing techniques in these pilot studies before proceeding on to the large series of *in vivo* implants.

From these pilots to date, with final histology still pending, we have determined that the constructs and cells are well tolerated and do not incite an inflammatory reaction. We have also learned that some differentiation needs to be induced prior to implantation for the construct to develop enough stiffness so that it is easy to manipulate surgically.

Ratio of differentiated to undifferentiated MDSCs

To address this latter issue, we have begun testing MDSCs with known stem cell, satellite, and muscle differentiation markers that will allow us to identify MDSCs at various stages of differentiation. We will then investigate the best ratio of differentiated to undifferentiated MDSCs for implantation. Some myoblast differentiation appears necessary to organize the matrix so that it is stiff enough to handle. However, we expect to find that it will be advantageous to retain a subset of the MDSC population in the undifferentiated state, so that these cells can continue to proliferate *in vivo*.

References

1. Cosgrove, B.D., Sacco, A., Gilbert, P.M., Blau, H.M. (2009) A home away from home: challenges and opportunities in engineering in vitro muscle satellite cell niches. *Differentiation* **78**:185-194.

2. Engler, A.J., Sen, S., Sweeney, H.L., Discher, D.E. (2006) Matrix elasticity directs stem cell lineage specification. *Cell* **126**: 677-689.

3. Gilbert, P.M., Havenstrite, K.L., Magnusson, K.E., Sacco, A., Leonardi, N.A., Kraft, P., Nguyen, N.K., Thrun, S., Lutolf, M.P., Blau, H.M. (2010) Substrate elasticity regulates skeletal muscle stem cell self-renewal in culture. *Science* **329**:1078-1081.

3. KEY RESEARCH ACCOMPLISHMENTS

Key research accomplishments, grouped by Task, are listed below.

Task 1

- Established the use of nylon (Nitex) meshes to provide a stable mechanical attachment for extracellular matrix hydrogels in microwell plate assays. Determined that 100 micron mesh/44% open space nylon (Nitex) mesh works adequately for the microwell plate assay application.

- Identified new polyvinyl alcohol (PVA) sponge materials (90 micron pore diameter) that will support HMW-HA hydrogels. These materials may offer improved gel adhesion over nylon mesh.

- Determined that the nylon (Nitex) mesh material can be used for a new application in this project – as suture anchors for the myobridge constructs (Task 11).

Task 2

- Performed and finished evaluations of microwell plate assay system for evaluating expression of GFP/FOXP3 in murine T cells. Established that the Packard fluorescence imager had the necessary sensitivity, but found that fluorescence signal from the cells was difficult to separate from backgrounds and that fluorescence analysis plates had cytotoxic properties. Our results indicated that an alternative, flow cytometry-based assay will be more effective at measuring the influence of HMW-HA hydrogels on GFP/FOXP3 expression by this cell type. The new assay uses a new form of disulfide bond-reducible HMW-HA that can be liquefied to free the cells for measurement.

Task 3

- Evaluated the effects of gelatin sponge inclusion on FOXP3 induction and found that the gelatin sponge adds structural integrity to hydrogels polymerized *in vitro* and that there is no functional disadvantage vis-à-vis FOXP3 induction to having the gelatin sponge present.

- Established methods to evaluate the capacity of HMW-HA to incorporate cytokines that stimulate FOXP3 expression by T cells. Showed that HMW-HA thiol-crosslinked hydrogels can bind IL-2 and IL-10 and can release these important immunomodulatory cytokines in a controlled manner, thereby indicating that HMW-HA hydrogels might be used as a means for local control of immune responses within wound and graft sites.

- Developed a new approach to incorporation of anti-CD3 and anti-CD28 antibodies in crosslinked HMW-HA hydrogels using biotinylated antibodies in conjunction with streptavidin. This new capability may provide a strong stimulus (via attachment of the antibodies to cell surface CD3 and CD28) that promotes the expansion and persistence of immunomodulatory regulatory T-cells within wound and graft sites. The presence of CD3 and CD28 signaling within the HMW-HA hydrogel could substantially enhance the immunomodulatory effects of IL-2 and IL-10 that are co-delivered within the same HMW-HA hydrogel.

- Demonstrated a significant effect of heparan sulfate (HS) on amplifying the influence of TGF-β and IL-2 on induction of FOXP3 by T-cell precursors. From these results, new HMW-HA hydrogel formulations were created that incorporated HS, anti-CD3, and anti-CD28 antibodies, IL-2, and TGF-β. These formulations stimulated a significant production of IL-10 from T-cell precursors and induced the formation of FOXP3+ regulatory T-cells from the precursor population.

Task 4

- Obtained Human Subjects approval for this Task and hired a Staff Scientist for the proposed experiments.

- Established the siRNA transfection method and developed siRNA sequences for 6 of 11 target genes.

- Adapted and optimized this transfection protocol for primary lymphocytes and confirmed that it resulted in highly efficient transfection, and high viability, in both T cells and B cells isolated from human PBMCs (data not shown).

- Established qPCR based assays to measure knockdown of PTPN22, PTPN2, and LAMIN A/C.

- Optimized protocol for gene-specific siRNA knockdown in primary CD4+ T cells.

- Validated 4 siRNAs specific for PTPN22 and PTPN2 that achieved effective knockdown. Experiments were performed that validated the time course of PTPN22 knockdown and quantitated protein reduction. It was found that knockdown of PTPN22 RNA persisted through 3 days but by day 4 RNA levels were returning to untransfected cell levels. Similar results were observed for PTPN2 knockdown. We observed that protein knockdown of PTPN2 lagged behind RNA knockdown by ~48 hours, with detectable knockdown at the protein level observed at 3 days after siRNA transfection.

- Started to evaluate the phenotypic effects of PTPN22 and PTPN2 knockdown in T-cells, determining the TCR signaling phenotype associated with PTPN22 siRNA knockdown in CD4+ T-cells and the IL-2 signaling phenotype associated with PTPN2 siRNAs knockdown in CD4+CD25hi T- cells.

- Expanded our evaluation of siRNAs to new target genes, including STAT3 and the IL-6 receptor. Demonstrated STAT3 siRNA knockdown in CD4+ T-cells.

Task 6

- Identified relevant siRNA sequences, received a set of siRNAs that target human TREM-2 and DAP12, and tested them in THP-1 cells, a monocyte-like cell line

- Initiated tests of additional antibodies for detection of TREM-2 and DAP12, so that we can measure knockdown at the protein level.

- Established a qPCR assay for measuring TREM-2 and DAP12 mRNA that we can use to evaluate the efficacy of knockdown in THP-1cells and cultured monocytes.

Task 7

- In initial experiments with wild-type and CD 18-deficient mice, demonstrated that CD18 inhibits TLR responses *in vivo* as well as *in vitro* in macrophages.

- Found that peritoneal macrophages from CD18-deficient mice produce more IL-6 and IL-12 p40 than those from wild-type mice, whereas the production of TNF was similar between the two genotypes. These data are similar to our findings with bone marrow-derived macrophages and further strengthen our conclusion that β2 integrins inhibit TLR signaling in a variety of macrophage populations.

- Investigated how BCAP inhibits TLR responses by comparing TLR-induced signal transduction in wild-type and BCAP-deficient macrophages, using SDS-PAGE and Western blot to examine the activation of the three MAPK signaling pathways and activation of the NF-κB pathway. It was determined that BCAP deficiency subtly affects the activation of MAPK pathways, but does not affect NF-κB activation.

Task 8

- Established a protocol to test the protective role of inflammatory cytokine blockade in humans prior to an inflammatory stimulus, obtained all necessary human subjects approvals, and enrolled 3 patients in our study. Our initial results suggested that IL-1 blockade with the IL-1 receptor agonist anakinra inhibited the generation of the inflammatory cytokine IL-8 (as measured in serum) that occurs during an experimentally-induced inflammatory stimulus (temporary hyperglycemia). These data indicate that we can successfully measure serum IL-8 in patients and that there may be a link between hyperglycemia and IL-8 levels. This research implies that our initial hypothesis that hyperglycemia is an appropriate stimulus to study inflammation is most likely correct.

- Samples on the patients that have completed the protocol have been stored and will be used to conduct the mechanistic assays detailed in the project.

- By the end of Year 1, 8 patients were recruited into the protocol. We anticipate being able to finish recruitment in Year 2 and to complete all sample analyses.

Task 9

- Produced 0.75 mm – 1 mm thick gelatin sponge prototypes crosslinked with either glutaraldehyde or EDC/NHS. Found that these sponges were mechanically strong, stable, and could be cut and perforated with relative ease. We also evaluated a commercially available crosslinked gelatin-based sponge as a supportive element for the CI.

- Began development of a new approach, based on calcium-crosslinked alginate hydrogels, for controlled release of cytokines and HMW-HA from the CI. We developed a method to create crosslinked alginate "macrospheres" of reproducible diameter (2 mm) and we established that the macrospheres could be used as a medium for prolonged, controlled release of soluble HMW-HA, which has been shown to have anti-inflammatory properties. We demonstrated that the rate of release of HMW-HA from alginate could be varied by altering the degree of crosslinking of the alginate with calcium. Significantly, we showed that HMW-HA could be released from alginate macrospheres in a linear fashion for extended periods of time (up to 3 months). In light of our finding that HMW-HA stimulates regulatory T-cells (Task 3), the capacity to deliver this molecule locally over a prolonged period via controlled release (using biocompatible alginate) may prove to be an effective means to control inflammation within wound sites and at the sites of regenerative tissue grafts.

- Extended our experiments to show that alginate macrospheres loaded with the angiogenic cytokine vascular endothelial growth factor (VEGF) could release this molecule in a controlled fashion over a period of at least 2 weeks *in vitro*. VEGF will likely prove to be an important component of the CI for its capacity to induce vascular growth within wound and graft sites.

- Began development of poly-L-lysine (PLL)-coated alginate macrospheres for controlled release of immunomodulatory cytokines of low molecular weight. Studies thus far have indicated that PLL coatings can effectively reduce or stop the release of HMW-HA from alginate for at least 28 days. Consequently, PLL coatings may be an effective method to modulate the kinetics of HMW-HA release from alginate and, potentially, control the release of immunomodulatory compounds such as TGF-β, IL-2, IL-10, and antibodies to CD3 and CD28. Extended, local delivery of these cytokines may be an effective way prolong the presence of FOXP3+ regulatory T-cells within wound and graft sites.

Task 10

- Established that unmodified Gelita-Spon™ gelatin sponge scaffold degrades after 3-4 days *in vivo* and evaluated the *in vivo* degradation rate of our HMW-HA hydrogels. By histology, we found evidence of a measured degradation of the HMW-HA hydrogel by macrophage-like "giant cells," associated with a fibrovascular cellular infiltrate. This degradation was accompanied by vascularization of the site. Notably, the process of degradation was accelerated by reducing the degree of thiol crosslinking of the hydrogel.

- Conducted studies to evaluate tissue responses to alginate macrospheres implanted *in vivo*. We determined by histology that alginate hydrogel is not immunogenic, does not support infiltration by cells, and does not biodegrade, at least over the short term. Therefore, the release kinetics of HMW-HA from alginate that we observe *in vitro* (Task 9) may be similar after the macrospheres are implanted *in vivo*. We also determined that incorporation of VEGF into alginate macrospheres induced an angiogenic response following implantation *in vivo*.

- Began studies *in vivo* to evaluate allo-immune responses to implanted, cytokine-loaded, crosslinked HMW-HA hydrogels (Extracel-HP) CIs. These allo-responses were induced by incorporating Balb/c-

29

strain mouse cell lysates into the CIs and implanting them into B6-strain mice. Our preliminary findings (by histology) suggested that there may be a protective effect on engrafted (islet) tissue; however, these experiments must be repeated to determine if the observations are valid.

Task 11

- The design and fabrication methods for novel "myobridge" constructs have been developed and incremental improvements are still evolving. The current constructs are now ready for cell seeding. This unique myobridge design has the potential to answer several challenges posed by *in vivo* implantation.

- Animal model development is progressing ahead of schedule. Pilot surgeries show that the procedure is well tolerated by rat subjects.

- *In vivo* pilot experiments with implants of acellular scaffold materials of different composition have been performed as baseline studies to examine leukocyte infiltration, host vascularization, and native muscle regenerative responses to different scaffold matrices. These experiments are still in progress, as the endpoints for tissue procurement have not yet been reached. The scaffolds that incorporate HMW-HA HyStem HP are the first use of this scaffold material for the support of skeletal myocytes.

- Histology methods are being optimized to determine the best means to fix and stain three-dimensional specimens with gel-like components and consistencies for histological assessments.

- Preliminary results from *in vivo* pilot experiments in rats show that the addition of the collagen scaffolds and HystemHP™ scaffolds seeded with/without rat MDSCs does not incite a notable inflammatory response in the host.

- Scaffolds with the cytoprotective additive CoPP have been piloted *in vitro* and, once final quantitative results are available, will be ready for *in vivo* testing. Matrices incorporating CoPP represent the first time that CoPP has been used as a scaffold additive for cytoprotection of seeded cells.

- Preliminary results from *in vitro* pilot experiments suggest that the addition of CoPP to scaffolds may not only improve cell survival, but also help muscle-derived stem cells retain their immaturity and proliferative potential. This finding will require further confirmation using differentiation markers. However, if borne out, this might, in turn, increase the proliferative potential of the MDSCs after *in vivo* implantation.

4. REPORTABLE OUTCOMES

Major funding applied for or awarded based on work supported by this award

Awarded Grants:

1. Department of Defense grant W81XWH-10-1-0789 *"Harnessing Autologous Stem Cells to Reconstruct Skeletal Muscle with Innervation Potential"* (M.D. Allen, Benaroya Research Institute, PI). Funding Dates 09/30/10 – 09/29/13. Funding Amount (total costs) $719,599. Concepts and results generated from Tasks 9 and 11 contributed to this proposal.

Pending Grants:

1. NIH/NIADDK DP3 proposal *"High-throughput analyses of Treg Cell Responses in T1D"* (D. Campbell, Benaroya Research Institute, PI). Funding Dates 09/30/11 – 09/29/16. Funding Amount (total costs) $8,230,105. Concepts and results generated from Tasks 1, 2, 3, 8, and 9 contributed to this proposal.

2. NIH/NIADDK DP3 proposal *"Stem-Cell Derived Beta Cells and Immune Evasion"* (V. Cirulli, University of Washington, PI). Funding Dates 09/30/11 – 09/29/16. Funding Amount (total costs) for the BRI subcontract is $1,574,125. Concepts and results generated from Tasks 2, 3, 9, and 10 contributed to this proposal.

3. NIH/NIADDK R01 proposal *"Tissue Integrity Cues and the Induction of TR1 Regulatory Cells"* (P.L. Bollyky, Benaroya Research Institute, PI). Funding Dates 09/30/11 – 09/29/16. Funding Amount (total costs) $2,287,500. Concepts and results generated from Tasks 2 and 3 contributed to this proposal.

4. Juvenile Diabetes Research Foundation (JDRF) Career Development Award proposal *"Vaccines to Induce Regulatory T-Cells for Autoimmune Diabetes"* (P.L. Bollyky, Benaroya Research Institute, PI). Funding Dates 09/30/11 – 9/29/16. Funding Amount (total costs) $500,000. Concepts and results generated from Tasks 2 and 3 contributed to this proposal.

5. Alliance for Lupus Research Pilot Grant *"The Impact of CSK and PTPN22 Genetic Variants on T and B Cell Signaling in SLE"* (K. Cerosaletti, Benaroya Research Institute, PI). Funding Dates 07/01/11 – 06/30/12. Funding Amount (total costs) $75,000. This proposal incorporated siRNA technology developed as part of Task 4.

6. NIH R01DK072457 competitive renewal *"Multiple Mechanisms of Impaired T Cell Regulation in T1D"* (J. Buckner, Benaroya Research Institute, PI). Funding Dates 09/01/11 – 08/31/16. Funding Amount (total costs) $2,248,750. This proposal incorporated siRNA technology developed as part of Task 4.

Abstracts

1. Kim, J., Wilson, H.-M., Kobashi, K., Allen, M.D. *Optimizing muscle stem cell constructs for pelvic floor reconstruction.* Accepted for presentation as a moderated poster at the Society for Urodynamics and Female Urology Annual Meeting, Basic Science Poster Session. March 1, 2011, Phoenix, AZ, USA.

2. Ni, M., MacFarlane, A.W. IV, Campbell, K.S., Hamerman, J.A. *BCAP mediated negative regulation of TLR signaling.* Regulatory Networks in Immunology and Inflammation Conference. June, 2010. Napa, CA, USA.

3. Yee, N., Hamerman J.A. *Inhibition of TLR Responses by β2 Integrins.* 14th International Congress of Immunology. August, 2010. Kobe, Japan.

Manuscripts

1. Bollyky, P.L., Wu, R.P., Falk, B.A., Lord, J.D., Long, S.A., Preisinger, A., Teng, B., Holt, G.E., Standifer, N.E., Braun, K.R., Xie, C., Samuels, P.L., Vernon, R.B., Gebe, J.A., Wight, T.N., Nepom, G.T. (2011) Extracellular matrix components guide TR1 regulatory T-cell induction from effector memory T-cell precursors. *Proc. Natl. Acad. Sci USA*, In Press.

Presentations

1. Bollyky, P.L. *High molecular weight hyaluronan actively promotes immune tolerance: mechanisms and potential applications.* Presented at the Gordon Proteoglycan Conference, July, 2010, Proctor, NH, USA.

2. Bollyky, P.L. *High molecular weight hyaluronan actively promotes immune tolerance: mechanisms and potential applications.* Presented at ISHAS (International Society for Hyaluronan Sciences), June, 2010, Kyoto, Japan.

3. Hamerman, J.A. *Regulation of inflammatory responses by ITAM signaling in macrophages.* Presented at "Bridging the Gap 2011" Symposium, 4th International Workshop on Cell Communication in Health and Disease, February, 2011, Medical University of Vienna, Vienna, Austria.

Patents and licenses applied for

1. *"Compositions and Methods for Modulating Immune Cells,"* P.L. Bollyky, G.T. Nepom, and M.G. Kinsella. International Patent Application No. PCT/US2010/060323, filed on 12/14/10.

2. *"In vivo upregulation of heme oxygenase-1 reduces skeletal muscle ischemia/reperfusion injury,"* M.D. Allen. Provisional patent application No. 61420791, filed with the US Patent and Trademark Office on 12/08/10.

5. CONCLUSION

5.1. Task Summaries

Tasks 1, 2, and 3

Tasks 1, 2, and 3 focus on the development of high molecular weight hyaluronan (HMW-HA)-based hydrogels engineered for controlled release of growth factors and cytokines. Tasks 1 and 2 are concerned with the creation of a microwell-based plate fluorescence assay to assess the effects of HMW-HA/collagen gel formulations on the induction of regulatory T-cell (Treg) function, as measured by expression of fluorescent GFP/FOXP3 gene product. Task 1 was successful, in that a miniaturized nylon mesh ring-supported hydrogel format to support dispersed T-cells for the microwell-based assay was developed. Task 2 evaluated the overall effectiveness of the microwell assay approach. From the Task 2 studies, it was determined that the assay was not effective in that it could not easily discriminate the GFP signal from the background. Also the plastic plates used in the assay were found to be cytotoxic to the T-cells. Follow-on studies under Task 2 resulted in the development of an alternative, flow cytometry-based assay for GFP/FOXP3 expression in T-cells. *This cytometric assay was critical to the generation of the Task 3 results. In a broader perspective, the assay will be a very useful tool for future studies of T-cell responses to specific extracellular matrix environments.*

Using the cytometric assay for GFP/FOXP3 expression reported above, Task 3 results showed that HMW-HA hydrogels could act as depots for release of IL-2 and IL-10, cytokines that are capable of stimulating the expansion and activity of Tregs, thereby supporting the hypothesis that HMW-HA hydrogels might be used as a means for local control of immune responses within wound and graft sites. Moreover, additional work under Task 3 resulted in the development of a method to couple anti-CD3 and anti-CD28 antibodies into the HMW-HA hydrogels (using biotinylated forms of the antibodies in conjunction with streptavidin). This capability allows the HMW-HA hydrogel to provide interacting T-cells with specific TCR signals that could act as potent stimulators of Treg expansion and persistence. These TCR signals would act in synergy with the signals provided by IL-2 and IL-10. The concept of providing multiple signals for Treg stimulation was further expanded by adding the extracellular matrix component heparan sulfate and the cytokine TGF-β to HMW-HA hydrogels. These bioactive molecules also promoted expansion of the Treg population. *Collectively, the results generated under Task 3 indicate that extracellular matrix hydrogels can be produced that incorporate a number of molecular species which may act in concert to provide potent signals for induction of Treg persistence and function.*

Task 4

Task 4 uses small interfering (si)RNAs introduced into naïve human CD4 T-cells to inhibit expression of target genes predicted to affect the generation or stability of Tregs, or alternatively, prevent the generation of inflammatory T-cells of the Th17 lineage. During Year 1, methods were established to achieve an efficient transfection of siRNAs into primary T and B cells, resulting in gene specific knockdown. Moreover, siRNAs for PTPN22, PTPN2, STAT3, and IL-6R were validated that inhibited expression of gene-specific RNA and protein. Functionally, siRNA mediated knockdown of PTPN22 expression was associated with increased TCR signaling in CD4 T-cells, as measured by calcium flux, which is consistent with the role of PTPN22 in dampening TCR signal strength. Knockdown of PTPN2 expression correlated with decreased IL-2 signaling, which phenocopies the effect of a genetic variant in PTPN2 that reduces PTPN2 expression. These findings have important implications: the PTPN22 siRNAs are an invaluable tool to reverse the immune phenotypes resulting from the 1858T genetic variant in PTPN22 that causes susceptibility to various autoimmune diseases. The PTPN2, STAT3, and IL-6R siRNAs can modulate IL-6 signaling which drives Th17 cell differentiation, which we are currently testing. In summary, good progress has been made in Year 1 towards the goal of modulating CD4 T-cell development using siRNAs. These experiments will be continued in Year 2.

Task 6

Task 6 is a component of Aim 1D, which assesses several endogenous inhibitors of the macrophage inflammatory response, TREM-2, BCAP, and β2 integrins, with the goal of developing strategies to down-modulate the macrophage inflammatory response as one of the multi-faceted approaches for cytoprotection examined in this project. The strategy of this Task is to knock down TREM-2 and DAP12 in human monocytes and monocyte-derived macrophages. So far, a set of siRNAs that target human TREM-2 and DAP12 have been tested in THP-1 cells, a human monocyte cell line. The studies have encountered difficulties with flow cytometry-based detection of TREM-2 and DAP12 to evaluate the efficacy of the knockdown. Therefore, efforts were shifted to set up a qPCR assay for measuring TREM-2 and DAP12 mRNA to evaluate the knockdown efficacy. This approach has been successful and the project is now in a position to evaluate the efficacy of the siRNAs targeting TREM-2 and DAP12 and their ability to modulate TNF production in THP-1 cells.

Task 7

The macrophage inflammatory response is potently activated by pattern recognition receptors that include the TLR family, which, when ligated, results in the secretion of pro-inflammatory cytokines, such as tumor necrosis factor, IL-12, and IL-6, as well as chemokines that attract other immune cells. One mechanism by which the inflammatory response is controlled is through endogenous inhibitors or negative regulators of TLR signaling, which include TREM-2 and DAP12, studied in Task 6. Additional inhibitors of TLR signaling include CD18 (β2 integrin) and BCAP, which are the subject of Task 7. In Year 1, the mechanism for BCAP-mediated inhibition of TLR responses was examined by comparing pathways activated in wild-type and BCAP-deficient macrophages. There was a slight enhancement of p38 MAPK and ERK phosphorylation after LPS treatment in BCAP-deficient macrophages in comparison with wild-type macrophages. In contrast, there was no change in the degradation of IkBα protein, the cytoplasmic inhibitor of NF-kB translocation to the nucleus. These results lead to the conclusion that BCAP-deficiency subtly affects the activation of MAPK pathways, but does not affect NF-kB activation.

To study the inhibition of TLR responses by β2 integrins, the activation of wild-type and CD18 KO thioglycollate-elicited macrophages was examined. It was found that, as with bone marrow-derived macrophages, thioglycollate-elicited macrophages from CD18 KO mice produce more IL-12 p40 and IL-6 than those from wild-type mice. Cytokine production *in vivo* was also compared in response to i.p. challenge with lipopolysaccharide, where it was found that more IL-12 p40, IL-6 and TNF were produced in sera of CD18 KO mice than wild-type mice. Therefore, it was concluded that β2 integrins inhibit TLR responses in a variety of macrophage populations, both *in vivo* and *ex vivo. Collectively, these results support the concept that engagement of β2 integrin on the macrophage surface may suppress pro-inflammatory behaviors. This finding is a first step toward the development of β2 integrin-targeted activating factors that could be incorporated into the CI in order to modulate the inflammatory activities of macrophages.*

Task 8

Cytokines mediate tissue injury and cellular dysfunction across a broad range of diseases. Specific cytokines, such as IL-6 and IL-8, are emerging as important mediators in sepsis and as prognostic indicators of systemic inflammation in patients with traumatic injury. Task 8 evaluates the protective role of inflammatory cytokine blockade in humans (induced by administration of an IL-1 receptor antagonist, anakinra) prior to an inflammatory stimulus (induced hyperglycemia). Task 8 activated in Quarter 2, and a significant amount of time was spent in establishing a human subjects protocol, receiving the necessary institutional human subjects approvals, and enrolling patients into the study. By the end of Year 1, eight patients were recruited into the protocol and full data sets had been collected on three patients. The results suggest that administration of IL-1 receptor antagonist does inhibit the generation of the inflammatory cytokine IL-8 (in serum) after the inflammatory stimulus. In Year 2, these studies will be expanded to the rest of the patient sample to determine if the observed trend is maintained. PBMCs are to be collected from all of the patients and will be phenotyped, with a focus on measurement of markers that respond to the presence of IL-8, which include IL-8 receptors and

CD11b integrin. *If the experiments performed under Task 8 can establish that inflammatory cytokine blockade (e.g., with IL-receptor antagonists) can effectively blunt inflammatory responses in humans, the results can be applied to the design of the CI, via incorporation of these antagonists into the HMW-HA hydrogel and/or the controlled release component.*

Task 9

Task 9 focuses on engineering and fabrication of the CI, which includes design of the supportive scaffold that will contain the HMW-HA hydrogel. Progress has been made developing gelatin sponge-based scaffolds that can be molded into a variety of shapes. Results indicate that gelatin sponge will likely be the material of choice based on its inherent biocompatibility. Stabilization of the gelatin sponge to control its rate of biodegradation can be accomplished by chemical crosslinking, which is best achieved with crosslinking agents of low toxicity, such as EDC/HNS. For the *in vivo* studies of CI function in rats proposed for Year 2, a degradation period of 4 weeks is probably sufficient. A similar period may be applicable for wound or graft applications in human patients.

In addition to work on the supportive scaffold for the CI, significant progress has been made toward the development of a device for controlled release of bioactive compounds that can be incorporated into the CI. Methods were developed to fabricate 2 mm diameter spheres (macrospheres) comprised of Ca^{++}-crosslinked alginate hydrogel. Subsequent experiments with the macrospheres demonstrated their capability for controlled release of angiogenic cytokines (VEGF) and HMW-HA, which has been shown to suppress inflammation and scar formation. *Importantly, it was shown that HMW-HA could be released in vitro from the alginate in a linear manner for extended periods of time, potentially up to 3 months, which suggests the potential of this method of drug delivery to provide long term suppression of inflammation and fibrosis in wound and graft sites.*

Also of significance was the finding that release of HMW-HA could be controlled by varying the degree of Ca^{++} crosslinking of the alginate or, alternatively, by coating the alginate with poly-L-lysine (PLL). *These methods of control may make it possible to tailor the rate and duration of HMW-HA administration to specific therapeutic requirements.* Finally, preliminary studies have shown that PLL coatings can influence the release rate of relatively low molecular weight compounds, such as antibodies, from alginate hydrogel. This finding, which requires additional experimentation to validate, may prove to be particularly important for the function of the CI, in that controlled delivery of TCR signaling molecules (e.g., anti-CD3/CD28) and cytokines from alginate could augment the stimulation provided by HMW-HA loaded with the same set of bioactive molecules (Task 3), thereby resulting in an extra, prolonged presence of these agents for maximal induction of Treg persistence and function.

Task 10

This Task begins to evaluate the responses of tissues *in vivo* to prototypical components of the CI. By histology, it was shown that HMW-HA (not supplemented with cytokines for Treg stimulation) undergoes a measured degradation by macrophage-like cells, which is accompanied by a fibrovascular cellular infiltrate and subsequent vascularization. Notably, the process of degradation is controllable; it can be accelerated by reducing the degree of thiol crosslinking of the hydrogel. Initial studies to evaluate allo-immune responses to implanted, cytokine-loaded HMW-HA hydrogels have been performed and have suggested a cytoprotective effect by the cytokines; however, additional experiments must be performed in Year 2 to validate the results.

Studies were also conducted that evaluated tissue responses to alginate macrospheres implanted *in vivo*. It was determined by histology that the alginate hydrogel is not immunogenic, does not support infiltration by cells, and does not biodegrade, at least over the short term. *Importantly, therefore, the prolonged release kinetics of HMW-HA from alginate observed in vitro (Task 9) may be maintained after the macrospheres are implanted in vivo.*

Task 11

Major loss of skeletal muscle from battlefield injuries and compartment syndrome is one of the most devastating, but common, problems encountered in military medicine. Although many devices and therapies

exist for correcting defects in bone, there is currently no way to generate suitable, functioning replacement tissue for skeletal muscle. Task 11 tackles the production and testing of "myobridges," composed of autologous muscle stem cells and natural matrix materials as a means to solve this problem.

During Year 1, we have significantly refined the design and the fabrication processes for the myobridges to address the specific requirements for an implantable construct. At the same time, we have been developing and testing candidate extracellular matrix-based scaffold materials themselves. As a first step, pilot studies have been undertaken in which an activator (CoPP) of the cytoprotective molecule heme oxygenase-1 has been added to scaffolds. The goal is to regulate the local micro-environment around the implant to maximize the survival and proliferation of seeded cells, to foster host vascularization, and to dampen the host innate immune response to the graft. This will be accomplished by choice of biomaterials and supplements within the myobridge graft, as well as by the presence of the CI.

5.2. "So What Section" – Evaluation of the Knowledge as a Scientific or Medical Product

This research program has a strongly translational focus – the primary objective being to develop a means to control the process of wound repair to achieve an optimal outcome where inflammation is controlled in a fashion that promotes healing and minimizes scarring. To achieve this objective, the problem is addressed using a number of novel approaches (represented by the stated Tasks) that are constituted to yield results that can be combined into a single device (medical product) that we refer to as the *Cytoprotective Implant* (CI). The overarching "theme" of each of these approaches – and of the CI as a whole – is that they make use of *natural* cellular processes and materials to achieve the desired result. These approaches include: (1) stimulation of the expansion, persistence, and activity of Tregs to make use of their native capacity to control the inflammatory process (*cytoprotection*); (2) the use of natural extracellular matrix (ECM) hydrogels, of specific formulations, as key stimulators of Treg-mediated cytoprotection; (3) the incorporation of strategies for local, controlled release of natural cytokines and ECM components from within the CI that will accelerate vascularization, provide long-lasting stimulation of Treg activity, and inhibit scar formation; and (4) the use of mechanically strong natural, biodegradable ECMs as a supportive scaffold for the ECM hydrogel components. We believe that use of natural cellular processes and materials to promote cytoprotection, combined with strategies of local delivery of bioactive agents, will optimize healing and minimize undesirable systemic side effects.

The four approaches listed above are concerned with development of the CI itself and include *basic science* studies to identify specific genes that control both the generation and functional phenotype of Tregs (Task 4), to characterize cell surface molecules that influence macrophage inflammatory responses (Tasks 6 and 7), and to evaluate the protective effects of inflammatory cytokine blockade (Task 8). The basic science studies are contributory to the development of the CI in that their results identify specific molecules that control immune cell behavior, which could be targeted by bioactive agents incorporated within the CI. In addition to the basic science studies, there are elements of *applied science and engineering*, which include the development of assays (Tasks 1 and 2) and the design of ECM-based materials that provide mechanical support, bioactivity, and controlled release functions for the CI (Tasks 3 and 9). The elements of basic science, applied science, and engineering are sufficient to produce a prototypical CI; however, the objective of generating a functional medical product will be substantially facilitated by the *in vivo* arms of the project, which evaluate tissue responses to components of the CI (Task 10) and which develop a novel, engineered tissue (the *myobridge*) (Task 11) that will serve as a test-bed for CI performance in the setting of a graft designed to reconstruct extensive skeletal muscle wounds. The myobridge is a critical element of the program: not only will it serve to evaluate CI performance in the scenario of wound repair and engraftment, but also it will, in its own right, be a highly useful medical device for treatment of skeletal muscle trauma. In Year 1, significant progress has been made in all of the active Tasks, and we are confident that these results, collectively, will contribute to the development of a CI that controls inflammation and improves healing.

6. REFERENCES

Task 3

1. Logeart-Avramoglou, D., Huynh, R., Chaubet, F., Sedel, L., Meunier, A. (2002) Interaction of specifically chemically modified dextrans with transforming growth factor beta1: potentiation of its biological activity. *Biochem. Pharmacol.* **63**: 129-137.

2. Blanquaert, F., Barritault, D., Caruelle, J.P. (1999) Effects of heparan-like polymers associated with growth factors on osteoblast proliferation and phenotype expression. *J. Biomed. Mater. Res.* **44**: 63-72.

Task 11

1. Cosgrove, B.D., Sacco, A., Gilbert, P.M., Blau, H.M. (2009) A home away from home: challenges and opportunities in engineering in vitro muscle satellite cell niches. *Differentiation* **78**:185-194.

2. Engler, A.J., Sen, S., Sweeney, H.L., Discher, D.E. (2006) Matrix elasticity directs stem cell lineage specification. *Cell* **126**: 677-689.

3. Gilbert, P.M., Havenstrite, K.L., Magnusson, K.E., Sacco, A., Leonardi, N.A., Kraft, P., Nguyen, N.K., Thrun, S., Lutolf, M.P., Blau, H.M. (2010) Substrate elasticity regulates skeletal muscle stem cell self-renewal in culture. *Science* **329**: 1078-1081.

7. APPENDICES

Abstracts

1. Kim, J., Wilson, H.-M., Kobashi, K., Allen, M.D. *Optimizing muscle stem cell constructs for pelvic floor reconstruction.* Accepted for presentation as a moderated poster at the Society for Urodynamics and Female Urology Annual Meeting, Basic Science Poster Session. March 1, 2011, Phoenix, AZ, USA.

2. Ni, M., MacFarlane, A.W. IV, Campbell, K.S., Hamerman, J.A. *BCAP mediated negative regulation of TLR signaling.* Regulatory Networks in Immunology and Inflammation Conference. June, 2010. Napa, CA, USA.

3. Yee, N., Hamerman, J.A. *Inhibition of TLR Responses by β2 Integrins.* 14th International Congress of Immunology. August, 2010. Kobe, Japan.

Manuscripts

1. Bollyky, P.L., Wu, R.P., Falk, B.A., Lord, J.D., Long, S.A., Preisinger, A., Teng, B., Holt, G.E., Standifer, N.E., Braun, K.R., Xie, C., Samuels, P.L., Vernon, R.B., Gebe, J.A., Wight, T.N., Nepom, G.T. (2011) Extracellular matrix components guide TR1 regulatory T-cell induction from effector memory T-cell precursors. *Proc. Natl. Acad. Sci USA*, in press.

**Society for Urodynamics and Female Urology
2011 Winter Meeting**
March 1–5, 2011
Arizona Biltmore Hotel
Phoenix, Arizona

Conclusion: Rho kinase activity showed significant difference between proximal and distal anterior vaginal wall. However, those differences were not correlated with age. Although this study has limitation of small sample size, this study suggest that vaginal pelvic floor relaxation is more severe in distal part of vaginal wall and age related change has little effect on muscle weakness but individual characteristics.

Table 1. Expression of Rho kinase activity in vaginal walls

		AP	AD	p-value
Patients (n=40)		1.60364	1.01718	<0.001
Age group	30's(3)	1.82298	1.04498	0.109
	40's(10)	1.78021	1.04899	0.013
	50's(10)	1.64923	1.10443	0.013
	60's(11)	1.44820	1.05571	0.075
	70's(6)	1.40868	0.73417	0.028

Poster #BS37
OPTIMIZING MUSCLE STEM CELL CONSTRUCTS FOR PELVIC FLOOR

Jason Kim, MD[1], Heather-Marie Wilson, PhD[2], Alvaro Lucioni, MD[1], Kathleen Kobashi, MD[1] and Margaret Allen, MD[2]
[1]Virginia Mason Medical Center, Seattle, WA; [2]Benaroya Research Institute, Seattle, WA
(Presented by: Jason Kim)

Introduction: Stem cells derived from autologous skeletal muscle biopsies are currently in clinical trials for stress urinary incontinence via transurethral injection. However, for use in pelvic floor reconstruction, it may be advantageous to organize implanted muscle-derived stem cells (MDSC) on biodegradable scaffolds. We sought to optimize the conditions for MDSC growth within candidate scaffolds by varying the seeding densities and scaffold composition.
**Methods:** MDSC were isolated from rat anterior tibialis using the pre-plating technique and were seeded at densities of between 2.2×10^6 cell/ml and 4.4×10^6 cell/ml onto Nitex frames using biodegradable scaffolds, which included 100% collagen and 95% collagen/5% Hystem-HP© (Glycosan Biosystems). Hystem-HP is a hydrogel designed to promote expansion of stem cells. A mixture of collagen and Hystem-HP was selected to achieve a balance, allowing a proportion of MDSC to proliferate, while still allowing differentiation of MDSC to muscle fibers. The fully polymerized constructs were incised on the long edges to induce uniaxial tension for cell and scaffold fiber alignment. These constructs were observed for up to 21 days.
Results: Seeding densities of 3.3×10^6 and 4.4×10^6 cell/ml caused excessive scaffold traction that resulted in construct dehiscence within 48 hr. However, a seeding density of 2.2×10^6 cell/ml provided stable constructs that did contract, but were able to remain intact for 21 days.
   At that density, H&E staining showed a higher cell density with a definite subpopulation of cells that retained proliferative ability (Fig. 1) in the constructs seeded on 95% collagen/5% Hystem-HP when compared to 100% collagen.
Conclusions: The preliminary findings here demonstrate that seeding density and scaffold composition are critical parameters to control in the generation of usable MDSC-seeded constructs suitable for in vivo implantation.

Figure 1: H&E Staining of MDSC Constructs
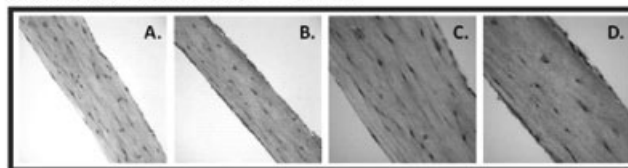
13 days
A. 100% collagen, 20x
B. 95% collagen/5% Hystem-HP, 20x
C. 100% collagen, 40x
D. 95% collagen/5% Hystem-HP, 40x

Poster #BS38
BONE MARROW MESENCHYMAL STROMAL CELL THERAPY FOR EXTERNAL URETHRAL SPHINCTER RESTORATION IN A RAT MODEL OF STRESS URINARY INCONTINENCE

Oleg Loutochin, MD, Lysanne Campeau, MD, Nicoletta Eliopoulos, PhD, Manaf Bouchentouf, PhD, Bertil Blok, MD, Jacques Galipeau, MD, PhD and Jacques Corcos, MD
JGH, Montreal, QC, Canada
(Presented by: Oleg Loutochin)

Introduction and Objectives: To assess the effect of intra−sphincteric injections of bone marrow mesenchymal stromal cells (MSCs) on Valsalva leak point pressure (VLPP) changes in an animal model of stress urinary incontinence (SUI).
Methods: Twenty-four female Sprague−Dawley rats underwent bilateral pudendal nerve section for SUI induction. Six rats were SUI controls, 6 received periurethral injection of Plasma-Lyte (SUI placebo control) and 12 were given periurethral injection of PKH26-labeled MSCs. Four weeks after injection, conscious cystometry was undertaken in animals and VLPP recorded. All groups were sacrificed, and frozen urethra sections were submitted to pathology assessment.
Results: Rat MSCs were positive for the cell surface antigens CD44, CD73, CD90, and RT1A, and negative for CD31, CD45, and RT1B, confirming their stem cell phenotype. In vitro, differentiated MSCs expressed α-smooth muscle actin (SMA) and desmin, markers of smooth and striated muscles. Immunohistochemistry of rat urethras revealed PKH26-labeled MSCs in situ and at the injection site. LPP was significantly improved in animals infused with MSCs. Mean LPP was 24.28 ± 1.47 cmH$_2$O in rats transplanted with MSCs and 16.21 ± 1.26 cmH$_2$O in SUI controls injected with Plasma Lyte ($P < 0.001$).
Conclusions: Bone marrow rat MSCs have the ability to differentiate and skew their phenotype towards smooth and striated muscles, as demonstrated by SMA up-regulation and desmin expression. Periurethral injection of MSCs in an animal model of SUI restored the damaged external urethral sphincter and significantly improved VLPP.

Poster #BS39
THE EFFECT OF DONOR AGE ON INDUCED PLURIPOTENT STEM CELLS FROM WOMEN WITH PELVIC FLOOR DISORDERS

Yan Wen, MD[1], Prachi Gujar, MS[2], Roger Jarvis, PhD[2], Thomas Baer, PhD[3], Renee Reijo Pera, PhD[2] and Bertha Chen, MD[4]
[1]Stanford University, Stanford, CA; [2]Institute for Stem Cell Biology and Regenerative Medicine, Stanford University,

BCAP mediated negative regulation of TLR signaling

Minjian Ni, Alexander W. MacFarlane, IV, Kerry S. Campbell, Jessica A. Hamerman

B cell adaptor for phosphoinositide 3-kinase (BCAP) was originally identified as an adaptor molecule that binds to the p85 subunit of phosphatidylinositol 3-kinase (PI3K). BCAP-deficient mice have decreased numbers of mature B cells and attenuated B cell function. Here we investigated the responses of BCAP deficient mice to stimulation through Toll-like receptors (TLRs). BCAP-deficient macrophages produced higher concentrations of inflammatory cytokines in response to a variety of pathogenic stimuli in vitro. BCAP-deficient mice produced more IL-12 in response to LPS in vivo. The PI3K inhibitor wortmannin enhanced TLR mediated proinflammatory cytokine production in wild type macrophages but not in BCAP-deficient macrophages. Our findings suggest that BCAP negatively regulates TLR mediated signaling in macrophages.

Inhibition of TLR Responses by β2 Integrins.

Nathan Yee and Jessica A. Hamerman

Abstract Early responses to microbes are mediated by the activation of Toll-like receptors (TLR) on macrophages and dendritic cells (DCs). Upon engagement of TLRs, macrophages and DCs produce proinflammatory cytokines, leading to activation of the immune system and microbial clearance. We have identified a novel role for β2 integrins in inhibiting TLR responses in macrophages and DCs. β2 integrins, which are best characterized as adhesion molecules mediating the firm adhesion of traveling leukocytes, are heterodimeric receptors consisting of the β2 subunit (CD18) bound to a member of the CD11 family of molecules. β2 integrin-deficient (CD18-/-) DCs display increased IL-12 p70, IL-6 and TNF production and cellular maturation in comparison with wild-type (WT) DCs following treatment with TLR agonists. CD18-/- macrophages produce increased IL-12 p40 upon TLR stimulation in comparison with WT macrophages. Direct ligation of β2 integrins via ICAM-1 reduces the stimulatory effects of LPS and CpG in WT macrophages and DCs. In addition, serum levels of pro-inflammatory cytokines are increased in CD18-/- mice following LPS injection in comparison with WT mice, demonstrating that β2 integrins are capable of inhibiting TLR activation *in vivo*. Macrophages and DCs share in common the expression of LFA-1 (CD11a/CD18) and Mac-1 (CD11b/CD18), however, CD11a-/- and CD11b-/- macrophages and DCs produce similar amounts of of pro-inflammatory cytokines following TLR stimulation as those from WT mice, arguing that LFA-1 and Mac-1 may share redundant functions in inhibiting TLR responses. These results demonstrate that signaling downstream of β2 integrins negatively regulate TLR activation in macrophages and DCs.

Extracellular matrix components guide TR1 regulatory T-cell induction

from effector memory T-cell precursors

Paul L. Bollyky*[†][‡], Rebecca P. Wu*, Ben A. Falk*, James D. Lord*, S. Alice Long*, Anton Preisinger*, Brandon Teng*, Gregory E. Holt[§], Nathan E. Standifer*, Kathy R. Braun*, Cindy Xie*, Peter L. Samuels*, Robert B. Vernon*, John A. Gebe*, Thomas N. Wight*, and Gerald T. Nepom*

* Benaroya Research Institute, 1201 Ninth Avenue, Seattle, WA 98101, USA.

[†] University of Washington Medical Center, Seattle, WA 98195, USA.

[‡] To whom correspondence should be addressed: pbollyky@benaroyaresearch.org

 P: (206) 583-6525 F: (206) 223-7543

[§] Division of Pulmonary, Critical Care and Sleep Medicine, University of Miami, Miami, FL 33136, USA

Non-standard abbreviations used: ECM; extra-cellular matrix, HA; hyaluronan, HMW-HA; high-molecular-weight hyaluronan, LMW-HA; low molecular weight hyaluronan, COL; collagen, HS; heparan sulfate. Classification

Character count (including spaces): 21,100

Running title: EXTRACELLULAR MATRIX AND TR1 INDUCTION

Classification: BIOLOGICAL SCIENCES: Immunology

ABSTRACT

We describe a novel role for extracellular matrix (ECM) as a biosensor for inflammatory microenvironments that plays a critical role in peripheral immune tolerance. We show that intact hyaluronan (HA) promotes induction of IL-10 producing TR1 regulatory cells from conventional T-cell precursors in both murine and human systems. This is, to our knowledge, the first description of an ECM component inducing regulatory T-cells. Intact HA, characteristic of healing tissues, promotes induction of TR1 capable of abrogating disease in an IL-10-dependent mouse colitis model while fragmentary HA, typical of inflamed tissues, does not, indicating a decisive role for tissue integrity in this system. The TR1 precursor cells in this system are CD4+CD62L-FoxP3-, suggesting that effector memory cells assume a regulatory phenotype when they encounter their cognate antigen in the context of intact HA. Matrix integrity cues might thereby play a central role in maintaining peripheral tolerance. This TR1 induction is mediated by CD44 crosslinking and signaling through p38 and ERK1/2. This induction is suppressed, also in a CD44-dependent manner, by osteopontin, a component of chronically inflamed ECM, indicating that CD44 signaling serves as a nexus for fate decisions regarding TR1 induction. Finally, we demonstrate that TR1 induction signals can be recapitulated using synthetic matrices. These results reveal important roles for the matrix microenvironment in immune regulation and suggest novel strategies for immunomodulation.

/body INTRODUCTION

The tissue microenvironment undergoes major changes following inflammatory stimuli and reverses these during the resolution of inflammation. In addition to a host of secreted soluble mediators, there are changes in the extracellular matrix component molecules themselves. We have studied the role of these changes as a communications bridge to the adaptive immune system, informing infiltrating lymphocytes regarding the tissue status and guiding subsequent response. In particular we have examined the interplay between components of the extracellular matrix and the TR1 regulatory T-cell subset.

TR1 are CD4+FOXP3- regulatory cells that play a crucial role in resolving inflammation and the maintaining peripheral immune tolerance (1). TR1 mediate contact-independent immune tolerance through the secretion of substantial amounts of IL-10 (2). While a diversity of experimental conditions have been used in TR1 induction (1)'(3)'(4)'(5)'(6)'(7)'(8) the specific progenitor population and governing factors *in vivo* are unclear(1). Given that TR1 cells are induced in peripheral tissues, presumably in response to local environmental cues, we hypothesized that extracellular matrix (ECM) components may play a role in TR1 induction.

We and others have identified a role for Hyaluronan (HA) interactions with CD44 as a biosensor of matrix integrity. HA is a long, highly charged disaccharide with prominent roles in structural biology, wound healing and immunology. The size of HA in a wound environment is known to correlate with the stage of injury and its resolution (9). Low-molecular weight forms of HA (LMW-HA) (<15 saccharides; <3 kDa) predominate during acute and persistent inflammation and have been demonstrated to be pro-

3

inflammatory and pro-angiogenic(10-12). Conversely intact high-molecular-weight HA

(HMW-HA) predominates in non-inflamed or healing tissues and is thought to be inert or

anti-inflammatory (9) We previously identified a role for HMW-HA in promoting the

persistence and function of established FoxP3+ natural T-reg (nTreg), (13-15). nTreg

are another regulatory T-cell subset that are thought to primarily arise in the thymus(16).

However, to our knowledge ECM components have not been implicated in the induction

of regulatory T-cells and there are no described roles for HA or CD44 in TR1 biology.

We report here that HMW-HA promotes TR1 induction from effector memory T-

cell precursors via interactions with CD44. We evaluate the functionality of TR1 cells

generated with co-stimulation from HMW-HA using an IL-10-dependent *in vivo* model of

colitis. We identify additional matrix components that intersect and modulate this

pathway, with CD44 signaling serving as a nexus for fate decisions regarding TR1

induction. Finally, we demonstrate that TR1 induction signals can be recapitulated

using synthetic matrices.

RESULTS

Intact HA promotes TR1 induction from effector memory T-cell precursors. To

ascertain the contribution of ECM components to TR1 induction, we devised a straight-

forward *in vitro* activation assay utilizing immobilized plate-bound ECM components

(**Supplemental Fig. 1A**). To exclude FOXP3+ nTreg, we utilized GFP/FOXP3 knock-in

mice and depleted the CD4+ T-cells isolated from these animals of GFP/FOXP3+ cells.

We tested a battery of ECM molecules and found that HMW-HA induced IL-10

production while type-1 collagen (COL), and fibrinogen (FB) did not (**Fig. 1A**). These

data indicate a specific role for HMW-HA in TR1 induction. HMW-HA promoted IL-10 production by CD4+GFP/FOXP3- T-cells while LMW-HA, generated from the same HMW-HA, did not. This was true at the level of protein (**Fig. 1B**) as well as at the RNA level (**Supplemental Fig. 1B**), implicating a decisive role for HA integrity in this system. Significant enhancement of other TH1, TH2 or TH17 cytokines tested was not observed (**Fig. 1C**). In particular, we did not observe enhanced production of IFN- γ, IL-2, or IL-5 (**Fig. 1C**) or TGF-β1 (**Supplemental Fig. 1C**), all cytokines variably associated with TR1 cells (1, 17). The effect of HMW-HA was dependent on the presence of a TCR stimulus, as HMW-HA in the absence of aCD3/28 was inert (**Supplemental Fig. 1D**). Cells induced to express IL-10 by HMW-HA co-stimulation retained this property even after being washed and re-stimulated with PHA/Ionomycin (**Supplemental Fig. 1E**).

We found that HMW-HA disproportionately promoted IL-10 production in the CD62L- fraction of CD4+ T-cells (**Fig. 1D**), which is to say the effector memory population. CD62L- T-cells are known to express CD44 at high levels(18), a phenotypic characteristic likely to be important in interactions with HMW-HA.

HA-induced TR1 are functional. The RAG.1-/- mouse colitis model is a well established system for evaluating IL-10-dependent regulatory T-cell effects. The infusion of CD4+CD45RB^{hi} naïve effector T-cells typically causes colitis in these animals while the co-infusion of regulatory T-cells abrogates colitis in an IL-10 dependent manner (19, 20). We used this model system to evaluate the regulatory capacity of TR1 cells induced with HMW-HA. Mice which received CD4+FoxP3 depleted T-cells activated with aCD3/28/HMW-HA exhibited significantly improved survival

relative to animals which received the same cells activated with aCD3/28 alone. Freshly

isolated CD4+GFP/FOXP3+ nTreg cells completely abrogated disease while infusion of

PBS alone in conjunction with the CD4+CD45RB^{hi} naïve effector T-cells led to the

demise of 90% of the animals in that experimental group (**Fig. 2A**). These effects on

survival occurred in conjunction with diminished colitis, as evidenced by evaluation

using a previously reported colitis scoring method (**Fig. 2B**). Representative colonic

sections are shown and clearly indicate the presence of healthy tissue with substantial

numbers of goblet cells in animals treated either with CD4+GFP/FOXP3+ nTreg or

CD4+GFP/FOXP3- cells treated with aCD3/28/HMW-HA. However in mice which

received either CD4+GFP/FOXP3- cells treated with aCD3/28 alone or PBS this normal

architecture is lost and pathologic features consistent with colitis are seen **(Fig. 2C)**.

HA induction of TR1 is CD44 dependent. CD44 is the primary cell-surface receptor

for HA (21). We found that CD44-/- mice exhibited significant impairment of IL-10 up-

regulation in response to HMW-HA (**Fig. 3A**). This indicates that CD44 is necessary for

HMW-HA mediated induction of IL-10. Consistent with this, costimulation of WT

CD4+GFP/FOXP- T-cells with plate-bound aCD44 robustly induced IL-10 production.

However, soluble aCD44 did not up-regulate IL-10 production, revealing a requirement

for CD44 cross-linking (**Fig. 3B**). The increase in IL-10 upon CD44 cross-linking was

still observed following normalization to tritiated thymidine incorporation levels (**Fig. 3C)**

dispelling the possibility that the IL-10 increase was an artifact of enhanced proliferation.

This increase in IL-10 was also seen at the level of mRNA expression, indicating that IL-

10 is actively produced in this system (**Supplemental Fig. 2A**). Unlike the cytokine

profile observed upon HMW-HA treatment, CD44 crosslinking also significantly increased TNFα and IFNγ (**Supplemental Fig. 2B**). This indicated that there are differences between HMW-HA and anti-CD44 antibody effects.

TR1 cells induced with CD44 cross-linking were functional, as demonstrated *in vitro* (**Fig. 3D**). Induced TR1 cells exhibited suppressive function comparable to freshly isolated nTreg. However, this suppressive function was lost when T-cells from IL-10-/- mice were utilized as a source of TR1 cells. Of note, CD44 co-stimulation of mouse CD4+GFP/FoxP3- cells failed to induce FoxP3 expression (**Supplemental Table 1**), indicating that the regulatory phenotype observed with these cells was not simply due to induction of FOXP3+ nTreg.

While CD44 facilitates signaling through numerous pathways, IL-10 production is reported to be primarily the product of signaling through MAP kinases, particularly those involving p38 and ERK1/2(22). Intracellular staining for IL-10 after CD44 co-stimulation identified enhanced IL-10 production that was lost upon addition of specific small molecule inhibitors of ERK1/2 (UO126) and p38 (SB202190) signaling but not upon inhibition of MEK1with PD98059 (**Figs. 3E and F**). This indicates that CD44 crosslinking promotes IL-10 production via a MAP kinase-dependent pathway. Consistent with this, we found that treatment with aCD44 together with a crosslinking antibody led to enhanced phosphorylation of both p38 and ERK1/2 which peaked 10 minutes post-activation (**Supplemental Figs. 3A and B**). If either the cross-linking antibody or the aCD44 antibody was left out enhanced phosphorylation of p38 and ERK1/2 was not seen (**Supplemental Figs. 3C and D**). The experiments in **Supplemental Fig. 3A-D** were performed using human CD4+CD25- T-cells; similar

results were seen with mouse cells (**Supplemental Figs. 3E and F**). As with HMW-HA, CD44 crosslinking disproportionately promoted IL-10 production in the CD62L-, effector memory population (**Fig. 3G**).

Intact HA promotes induction of human TR1. Co-stimulation of human CD4+CD25- T-cells with either HMW-HA or anti-CD44 antibodies significantly increased IL-10 production (**Supplemental Fig. 4A**) and generated functional TR1 cells (**Supplemental Fig. 4B**) but did not promote induction of Foxp3 (**Supplemental Fig. 4C**). These data thereby establish that human conventional T-cells also use HMW-HA and CD44 co-stimulation as cues to assume a TR1-like regulatory phenotype.

Exogenous IL-2 boosts HMW-HA induced IL-10 production. IL-2 has been reported to promote IL-10 production by TR1 cells in a STAT5-dependent manner (23). We found that exogenous IL-2 did indeed significantly increase IL-10 production in the presence of plate-bound HMW-HA (**Supplemental Fig. 5**). However, the enhanced IL-10 production seen upon IL-2 addition to the aCD3/28 condition did not reach statistical significance, leading us to suspect that the beneficial effect of IL-2 on IL-10 production may not be relevant at the low levels of TCR activation used in our system.

Osteopontin abrogates HA TR1 induction in a CD44 dependent manner. In healing tissues HA typically exists in the context of a complex ECM. We therefore asked whether other ECM components which are also CD44 ligands might impact the HA-mediated effect on TR1 induction described here. Osteopontin (OPN) is a matrix

8

glycoprotein found in abundance in chronic inflammation and known to exacerbate autoimmunity in several disease models (24-28). Given that OPN is known to decrease IL-10 production in a variety of settings and is a known ligand of CD44(25, 29) we explored the hypothesis that OPN inhibits HA-mediated TR1 induction. We observed that OPN decreased basal levels of IL-10 production seen upon aCD3/28 activation alone and negated the increase in IL-10 production seen upon HMW-HA co-stimulation in a dose-dependent manner (**Fig. 4A**). This was also the case on the level of mRNA expression (**Supplemental Fig. 6A**).   OPN inhibited HMW-HA-mediated IL-10 production to an equivalent extent irrespective of IL-2 supplementation (**Supplemental Fig. 6B**), indicating that the effect of OPN on IL-10 production occurs distal to or independent of STAT5 signaling.

OPN effects are known to be mediated by interactions with both CD44 as well as to the αVβ3 integrin receptor, to which it binds via an RGD motif (29). We observed that the decrease in basal IL-10 production upon OPN treatment was lost in CD44-/- mice (**Fig. 4B**) implicating CD44 in OPN effects on IL-10. Addition of RGD peptide, but not RGE control peptide, blocked the impact suppression of IL-10 production by OPN (**Fig. 4C**). Moreover, an activating antibody directed at the β3 integrin receptor subunit also negated the effect of HMW-HA (**Fig. 4D**).   These data implicate a role for both CD44 and integrin receptor signaling in OPN effects on HA-mediated IL-10 production and indicate a nexus for regulatory control of the TR1 pathway by ECM components.

A synthetic ECM hydrogel promotes IL-10 production through TR1 induction. We explored the potential of biomimetics of HA-containing matrix to induce Il-10 production.

Extracel® is a HMW-HA and collagen-based hydrogel preparation(30) which we modified to deliver a polyclonal antigenic stimulus through the addition of streptavidin and biotinylated aCD3 prior to polymerization. A schematic of this hydrogel design, referred to henceforth as an HA/COL gel, is shown (**Figure 5A**). CD4+GFP/FOXP3- T-cells activated using this platform produced IL-10 in comparable quantities to that seen with plate-bound activation while Matrigel or a fibrin hydrogel did not promote IL-10 induction (**Figure 5B**).

In tissues, IL-2 is associated with sulfated proteoglycans such as heparan sulphate (HS) possibly prolonging its half-life (31, 32). We therefore asked whether a synthetic matrix containing HS could be used to deliver IL-2 in conjunction with the other signals necessary for TR1 induction. Extracel HP®, a hydrogel preparation which incorporates HS in addition to collagen and HMW-HA (henceforth referred to as an HA/HS/COL gel) engendered equivalent IL-10 production in the absence of exogenous IL-2. However, upon IL-2 supplementation the HA/HS/COL gel engendered significantly increased IL-10 over the HA gel or plate-bound HMW-HA (**Figure 6C and D**). This is consistent with other reports of enhanced functionality of cytokines in HS-bound form (33, 34). IL-2-mediated enhancement of TR1 induction using synthetic matrices was not associated with an increase in other Th1, Th2 or TH17 cytokines (**Figure 6E**). While IL-2 has been previously demonstrated to bind to HS (35), we confirmed that a HA/HS/COL gel can retain IL-2 (**Supplemental Figure 7**).

DISCUSSION

The local inflammatory milieu and the ECM in particular are underappreciated partners of the adaptive immune response,. Herein we provide evidence of ECM modulation and control of TR1 cells, a key immunoregulatory cell in many peripheral tissues. Using both mouse and human cells, we show that intact HA promotes induction of IL-10 producing TR1 regulatory cells from conventional T-cell precursors and that these function *in vivo*.

The exclusivity with which HMW-HA treatment and particularly HMW-HA-based hydrogels promoted IL-10 production is noteworthy. In particular, we did not observe enhanced production of IFN- γ, IL-2, or IL-5, cytokines variably associated with TR1 cells (1, 17). Nor did we observe induction of FOXP3 or TGF-β1, molecules associated with other regulatory T-cell subsets. However, crosslinking of CD44 using plate-bound antibodies enhanced production of IFN-γ and TNF-α in addition to IL-10. These distinctions indicate differences between HMW-HA and anti-CD44 antibody effects. These may reflect differences in signal strength or the broader variety of CD44 variant isoforms crosslinked by the anti-CD44 antibody. Given that CD44v isoforms are thought to possess diverse ECM ligand specificities (36), it may be that other ECM components, accessory molecules known to interact with these components, and other receptors known to partner with CD44 may engender distinct patterns of cytokines in concert with IL-10 in a highly contextual and specific manner.

The TR1 progenitor cells in this system are CD4+CD62L- effector memory cells. This suggests that these cells have previously encountered their cognate antigens and assume a regulatory phenotype when they do so again in the context of HMW-HA. Moreover, HMW-HA treatment engendered a regulatory phenotype which persisted

11

even after they were withdrawn from contact with HMW-HA. Matrix integrity cues might thereby play a central role in maintaining peripheral tolerance to self antigens.

We identify two levels of regulation which modulate the capability of HA to induce TR1 regulatory cells. The first is the size of HA in the system. While HMW-HA, characteristic of healing or uninjured tissues, promotes IL-10 production, fragmentary LMW-HA, indicative of active tissue injury, does not, indicating a decisive role for HA integrity in TR1 induction. It is known that the length of HA chains dictates their ability to crosslink multiple CD44 receptors on the cell surface (37) and this crosslinking is critical to a number of CD44-mediated functions (38-40). The requirement for CD44 crosslinking in this system provides a potential mechanistic explanation tying TR1 induction to the inflammatory milieu *in vivo*.

A second level of control over HMW-HA induction of TR1 cells is the influence of OPN, a matrix glycoprotein found in abundance in many settings of chronic inflammation and autoimmunity (27, 28). Our data indicate that OPN overrides HMW-HA-mediated TR1 induction in a dose dependent manner via interactions with both CD44 and integrin receptors. These data point to a central role for CD44 in fate decisions regarding of TR1 induction. Furthermore, we demonstrate that the effect of OPN can be replicated with an antibody directed against β3 integrin. Our data suggest that interventions directed at OPN interactions with αVβ3 would be an appropriate target for intervention in autoimmune settings where OPN promotes disease. These data indicate a nexus for regulatory control of the TR1 pathway by ECM components.

Building upon our findings, we have developed synthetic matrix platforms capable of providing the necessary cues for TR1 induction *in vivo*. These platforms

12

capitalize on the shared capacity of intact HA and an HA-based hydrogel to induce TR1. In this context, the hydrogel can be regarded as a synthetic biomimetic of uninjured ECM. The use of synthetic matrices to induce TR1 points towards novel strategies for immunomodulation.

The key role of ECM molecular cues in guiding adaptive immune regulatory decisions, as demonstrated in this study, reflects an important communication pathway that is not evident from conventional *in vitro* laboratory studies. Introducing biomimetics of this pathway for *in vivo* use may expand opportunities to exploit ECM components as biosensors of tissue integrity and signals for immune response.

MATERIALS AND METHODS

Induction of TR1 cells and controls: CD4+GFP/FoxP3+ T-cells ($2x10^5$) were activated for 96 hours on plates initially coated with anti-CD3 (0.5µg/ml) +/- CD44 antibody (1µg/ml), washed, and then subsequently coated with either 0.2mg/ml BSA-conjugated HMW-HA or 10% BSA. Where indicated specific inhibitors of p38 (SB202190, A.G. Scientific), MEK1 (PD98059, A.G. Scientific), and ERK1/2 (UO126, Sigma Aldrich)(10mM), soluble LMW-HA (20µg/ml), or OPN (R&D Systems)(1-5µg/ml). RGD peptide (sequence GRGDNP) and RGE peptide (sequence GRGENP)(Sigma Genosys) were both used at 0.1µg/ml and added 10 minutes prior to the addition of OPN. After 96 hours cells and supernatants were collected for analysis.

TR1 induction using hydrogels: Extracel® and Extracel-HP® hydrogels from Glycosan Biosystems Inc. were used per the manufacturer's instructions. Biotinylated anti-CD3 antibody (BD Biosciences) and streptavidin (Sigma Aldrich) were both added

at 10µg/ml. CD28 antibodies (1.0µg/ml) were either added in biotinylated or in soluble

form. $2x10^5$ cells were layered on gels of 25µl volume following their polymerization.

Additional information on materials and methods is included in the supplemental data.

ACKNOWLEDGMENTS

AUTHOR CONTRIBUTIONS

PLB, JAG, and GTN designed the experiments. RBV and TNW provided reagents and

technical expertise. PLB, RPW, BAF, FX, AP, BT, KRB, and PLS performed the

experiments. PLB, JDL, SAL, GEH, NES, TNW and GTN contributed to data analysis.

PLB and GTN wrote the manuscript.

References

Reference List

1. Roncarolo, M. G., et al. (2006) Interleukin-10-secreting type 1 regulatory T cells in rodents and humans.*Immunol. Rev.* **212**, 28-50.

2. Vieira, P. L. , et al. (2004) IL-10-secreting regulatory T cells do not express Foxp3 but have comparable regulatory function to naturally occurring CD4+CD25+ regulatory T cells.*J. Immunol.* **172**, 5986-5993.

3. Groux, H., et al. (1997) A CD4+ T-cell subset inhibits antigen-specific T-cell responses and prevents colitis. *Nature* **389**, 737-742.

4. Awasthi, A., et al.. (2007) A dominant function for interleukin 27 in generating interleukin 10-producing anti-inflammatory T cells.*Nat. Immunol.* **8**, 1380-1389.

5. Pedersen, A. E., Gad, M., Walter, M. R., & Claesson, M. H. (2004) Induction of regulatory dendritic cells by dexamethasone and 1alpha,25-Dihydroxyvitamin D(3)*Immunol. Lett.* **91**, 63-69.

6. Kemper, C., et al. (2003) Activation of human CD4+ cells with CD3 and CD46 induces a T-regulatory cell 1 phenotype.*Nature* **421**, 388-392.

7. Levings, M. K, et al. (2005) Differentiation of Tr1 cells by immature dendritic cells requires IL-10 but not CD25+CD4+ Tr cells.*Blood* **105**, 1162-1169.

8. Hawrylowicz, C. M. & O'Garra, A. (2005) Potential role of interleukin-10-secreting regulatory T cells in allergy and asthma.*Nat. Rev. Immunol.* **5**, 271-283.

9. Stern, R., Asari, A. A., & Sugahara, K. N. (2006) Hyaluronan fragments: an information-rich system *Eur. J. Cell Biol.* **85**, 699-715.

10. Jiang, D., et al. (2005) Regulation of lung injury and repair by Toll-like receptors and hyaluronan.*Nat. Med.* **11**, 1173-1179.

11. Termeer, C., et al. (2002) Oligosaccharides of Hyaluronan activate dendritic cells via toll-like receptor 4.*J. Exp. Med.* **195**, 99-111.

12. Powell, J. D. & Horton, M. R. (2005) Threat matrix: low-molecular-weight hyaluronan (HA) as a danger signal. *Immunol. Res.* **31**, 207-218.

13. Bollyky, P. L., et al. (2007) Cutting edge: high molecular weight hyaluronan promotes the suppressive effects of CD4+CD25+ regulatory T cells.*J. Immunol.* **179**, 744-747.

14. Bollyky, P. L., et al. (2009) CD44 costimulation promotes FoxP3+ regulatory T cell persistence and function via production of IL-2, IL-10, and TGF-beta.*J. Immunol.* **183**, 2232-2241.

15. Bollyky, P. L., et al. (2009) Intact extracellular matrix and the maintenance of immune tolerance: high molecular weight hyaluronan promotes persistence of induced CD4+CD25+ regulatory T cells.*J. Leukoc. Biol.* **86**, 567-572.

16. Sakaguchi, S., Setoguchi, R., Yagi, H., & Nomura, T. (2006) Naturally arising Foxp3-expressing CD25+CD4+ regulatory T cells in self-tolerance and autoimmune disease.*Curr. Top. Microbiol. Immunol.* **305**, 51-66.

17. O'Garra, A., Vieira, P. L., Vieira, P., & Goldfeld, A. E. (2004) IL-10-producing and naturally occurring CD4+ Tregs: limiting collateral damage.*J. Clin. Invest* **114**, 1372-1378.

18. Budd, R. C., et al. (1987) Distinction of virgin and memory T lymphocytes. Stable acquisition of the Pgp-1 glycoprotein concomitant with antigenic stimulation.*J. Immunol.* **138**, 3120-3129.

19. Asseman, C., Mauze, S., Leach, M. W., Coffman, R. L., & Powrie, F. (1999) An essential role for interleukin 10 in the function of regulatory T cells that inhibit intestinal inflammation. *J. Exp. Med.* **190**, 995-1004.

20. Groux, H., et al. (1997) A CD4+ T-cell subset inhibits antigen-specific T-cell responses and prevents colitis.*Nature* **389**, 737-742.

21. Laurent, T. C. & Fraser, J. R. (1992) Hyaluronan *FASEB J.* **6**, 2397-2404.

22. Saraiva, M. & O'Garra, A. (2010) The regulation of IL-10 production by immune cells. *Nat. Rev. Immunol.* **10**, 170-181.

23. Tsuji-Takayama, K., et al. (2008) The production of IL-10 by human regulatory T cells is enhanced by IL-2 through a STAT5-responsive intronic enhancer in the IL-10 locus.*J. Immunol.* **181**, 3897-3905.

24. Hur, E. M., et al. (2007) Osteopontin-induced relapse and progression of autoimmune brain disease through enhanced survival of activated T cells.*Nat. Immunol.* **8**, 74-83.

25. Heilmann, K., et al. (2008) Osteopontin as two-sided mediator of intestinal inflammation.*J. Cell Mol. Med.*

26. Fisher, L. W. & Fedarko, N. S. (2003) Six genes expressed in bones and teeth encode the current members of the SIBLING family of proteins. *Connect. Tissue Res.* **44 Suppl 1**, 33-40.

27. Wang, K. X. & Denhardt, D. T. (2008) Osteopontin: role in immune regulation and stress responses.*Cytokine Growth Factor Rev.* **19**, 333-345.

28. Cantor, H. & Shinohara, M. L. (2009) Regulation of T-helper-cell lineage development by osteopontin: the inside story. *Nat. Rev. Immunol.* **9**, 137-141.

29. Ashkar, S., et al. (2000) Eta-1 (osteopontin): an early component of type-1 (cell-mediated) immunity. *Science* **287**, 860-864.

30. Prestwich, G. D., et al. (2006) Injectable synthetic extracellular matrices for tissue engineering and repair.*Adv. Exp. Med. Biol.* **585**, 125-133.

31. Najjam, S., et al. (1998) Further characterization of the binding of human recombinant interleukin 2 to heparin and identification of putative binding sites.*Glycobiology* **8**, 509-516.

32. Wrenshall, L. E., Platt, J. L., Stevens, E. T., Wight, T. N., & Miller, J. D. (2003) Propagation and control of T cell responses by heparan sulfate-bound IL-2.*J. Immunol.* **170**, 5470-5474.

33. Schonherr, E. & Hausser, H. J. (2000) Extracellular matrix and cytokines: a functional unit. *Dev. Immunol.* **7**, 89-101.

34. Lortat-Jacob, H. (2009) The molecular basis and functional implications of chemokine interactions with heparan sulphate.*Curr. Opin. Struct. Biol.* **19**, 543-548.

35. Najjam, S., Gibbs, R. V., Gordon, M. Y., & Rider, C. C. (1997) Characterization of human recombinant interleukin 2 binding to heparin and heparan sulfate using an ELISA approach. *Cytokine* **9**, 1013-1022.

36. Pure, E. & Cuff, C. A. (2001) A crucial role for CD44 in inflammation. *Trends Mol. Med.* **7**, 213-221.

37. Lesley, J., Hascall, V. C., Tammi, M., & Hyman, R. (2000) Hyaluronan binding by cell surface CD44. *J. Biol. Chem.* **275**, 26967-26975.

38. Fujii, Y., Fujii, K., Nakano, K., & Tanaka, Y. (2003) Crosslinking of CD44 on human osteoblastic cells upregulates ICAM-1 and VCAM-1.*FEBS Lett.* **539**, 45-50.

39. Huet, S., et al. (1989) CD44 contributes to T cell activation *J. Immunol.* **143**, 798-801.

40. Wyant, T. L., et al. (2005) Mouse B cell activation is inhibited by CD44 cross-linking. *Immunol. Invest* **34**, 399-416.

41. Ostanin, D. V., et al. (2009) T cell transfer model of chronic colitis: concepts, considerations, and tricks of the trade. *Am. J. Physiol Gastrointest. Liver Physiol* **296**, G135-G146.

FIGURE LEGENDS

Figure 1. HMW-HA costimulation induces a TR1-like phenotype in CD4+GFP/FoxP3-CD62L- effector memory T-cells. A. IL-10 production upon activation with aCD3/28 alone or in conjunction with the ECM components HMW-HA, collagen (COL), and fibrinogen (FB). **B.** Effects of HMW-HA or LMW-HA treatment on IL-10 production. **C**. Fold change in TH1, TH2 and TH17 cytokines levels upon HMW-HA co-stimulation. N = 5 experiments each for **A-C, D.** Fold change in IL-10

concentration in cell culture supernatants taken from mouse CD4+GFP/FoxP3- T-cells sorted on the basis of CD62L expression and activated +/- HMW-HA. Data were normalized to the aCD3/28 condition of the CD62L- population with this value equaling 1 for each experiment (N = 4 independent experiments).

Figure 2. Generated TR1 can suppress the development of colitis. A. Impact of putative TR1 and controls on survival in an IL-10-dependent mouse colitis model. N = an average of 12 mice per group. **B**. Histology scores for the colitis seen in the mice in (**A**). **C.** Representative histology of colon sections taken from the mice in (**A**.) demonstrating goblet cell depletion, inflammatory infiltrate, epithelial shedding and crypt micro-abscesses only in mice receiving aCD3/28 treated T-cells or PBS.
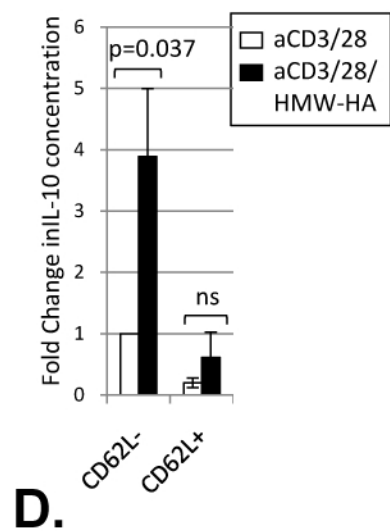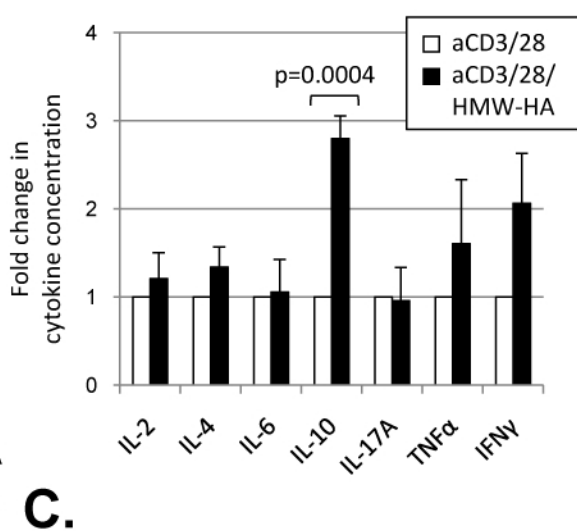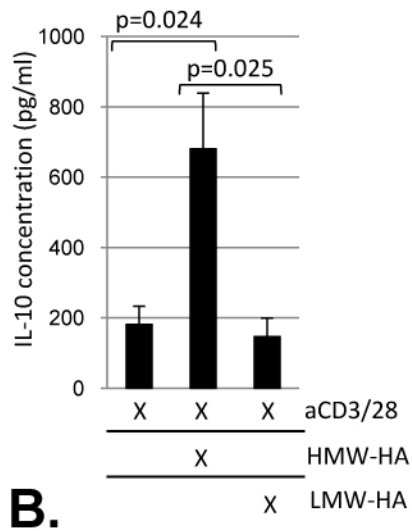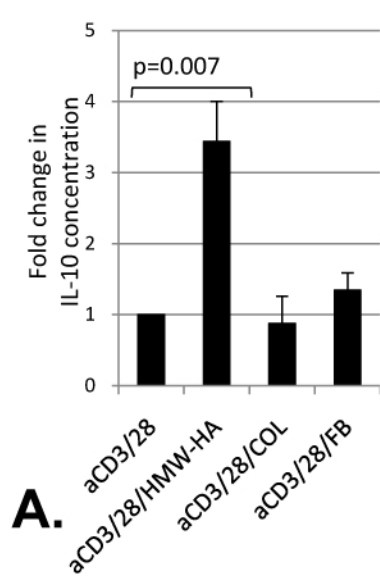
Figure 3. CD44 cross-linking promotes MAP kinase-dependent IL-10 production. A. HMW-HA-induced IL-10 production using WT or CD44-/- precursor T-cells (N = 7 experiments).   **B.** IL-10 production upon costimulation with plate-bound or soluble aCD44 (N = 5 experiments). **C.** Effects of CD44 cross-linking on IL-10 production, normalized to proliferation. Data are expressed as pg/ml of IL-10 produced on a per-CPM basis. **D**. Suppression assay utilizing TR1 cells induced with aCD44 costimulation. **C** and **D** are each representative of two experiments. Representative Intracellular staining (**E**) and fold change in IL-10 production **(F)** following treatment with aCD44 and selective inhibitors of p38 (SB202190), ERK1/2 (UO126), and MEK (PD98059)(N = 5 experiments). **G.** Fold change in IL-10 concentration in cell culture supernatants taken from mouse CD4+GFP/FoxP3- T-cells sorted on the basis of CD62L expression and activated +/- HMW-HA. Data were normalized to the aCD3/28 condition of the CD62L-
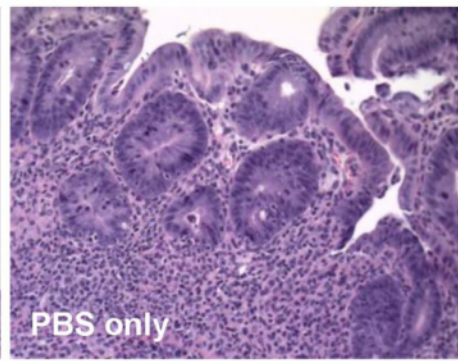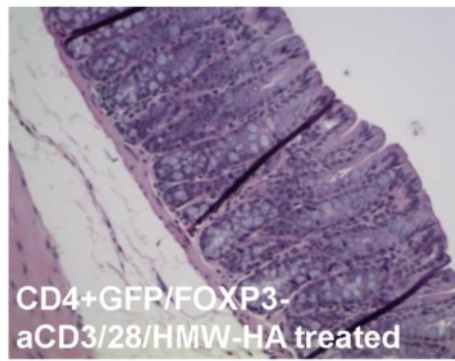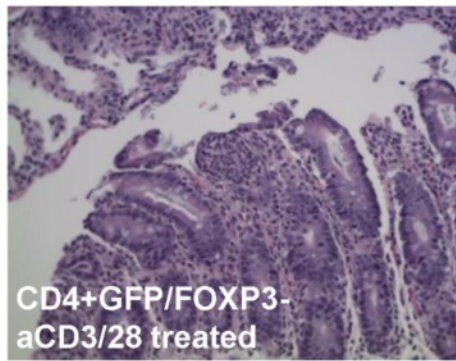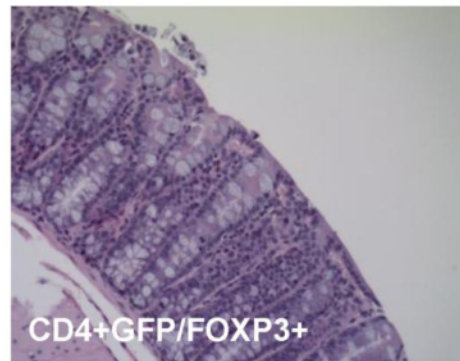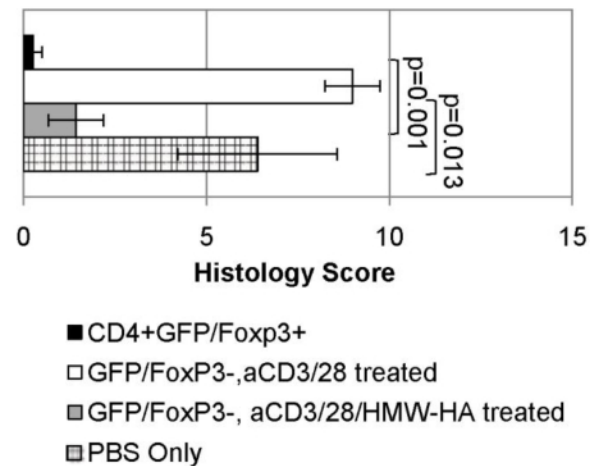
population with this value equaling 1 for each experiment (N = 4 independent experiments).

Figure 4. OPN abrogates HMW-HA mediated IL-10 production. A. Effects of OPN concentration on IL-10 production (N = 3 experiments). **B.** Effect of OPN on IL-10 production by WT and CD44-/- T-cells. **C.** Effect of RGD or RGE peptides on OPN-mediated suppression of IL-10 production. Data for **B** and **C** are each representative of three experiments. **D.** Effects of integrin antibodies on HMW-HA-mediated IL-10 production (N = 5 experiments).

Figure 5. A synthetic matrix promotes TR1 induction. A. Schematic of a hydrogel which delivers a set of stimuli capable of inducing TR1 from conventional T-cell precursors. **B.** IL-10 production following plate-based or hydrogel-based activation (n = 5 experiments). **C.** The impact of supplemental IL-2 on IL-10 production in the setting of plate-based or HA/COL or HA/COL/HS hydrogels (n = 5 experiments). **D.** Representative intracellular staining for IL-10 under these same conditions. **E.** Levels of TH1, TH2 and TH17 cytokines upon hydrogel-based activation (n = 3 experiments).

A. Fold change in IL-10 concentration vs aCD3/28, aCD3/28/HMW-HA, aCD3/28/COL, aCD3/28/FB (p=0.007)

B. IL-10 concentration (pg/ml) for aCD3/28, HMW-HA, LMW-HA conditions (p=0.024, p=0.025)

C. Fold change in cytokine concentration for IL-2, IL-4, IL-6, IL-10, IL-17A, TNFα, IFNγ comparing aCD3/28 and aCD3/28/HMW-HA (p=0.0004)

D. Fold Change in IL-10 concentration for CD62L- and CD62L+ comparing aCD3/28 and aCD3/28/HMW-HA (p=0.037, ns)

A.

B.

C.

A.

B.

C.

D.

E.

F.

G.

A.

B.

C.

D.

A.
- ─── HA
- ─── COL
- ⬤ Streptavidin
- ⚕ Biotinylated anti-CD3

B.
IL-10 concentration (pg/ml)

p=0.002
p=0.034

PBS, HMW-HA, HA/COL Gel, Matrigel, Fibrin Gel

Plate-bound aCD3 Soluble aC28 | Streptavidin, Biotinylated aCD3, Soluble aCD28

C.
IL-10 concentration (pg/ml)

☐ Media   ■ IL-2

p=0.037
p=0.015
p=0.015
p=0.047

PBS, HMW-HA, HA/COL Gel, HA/HS/COL Gel

Plate-bound aCD3 Soluble aC28 | Streptavidin, Biotinylated aCD3, Soluble aCD28

D.
Plate-bound aCD3; Soluble aCD28
IL-2 20 IU/ml

PBS
0.5   1.6
7.6   90

HMW-HA
1   8.3
5.5   85

Streptavidin, Biotinylated aCD3,
Soluble aCD28, IL-2 20 IU/ml

HA/COL Gel
1.6   9.2
5   84

HA/HS/COL gel
1.5   21
3.8   74

IL-10 APC (y-axis)
CD4-PerCP (x-axis)

E.
pg/ml

☐ PBS (Plate-bound activation)
▨ HA/COL Gel
■ HA/HS/COL Gel

p=0.041
p=0.012

IL-4, IL-10, IL-6, IL-17A, TNFα, IFNγ